



Johanna Pirchner, BSc

# **Establishing Lambda RED Recombineering for Efficient Genome Engineering of *Cupriavidus necator* H16**

## **MASTER'S THESIS**

to achieve the university degree of

Diplom-Ingenieurin

Master's degree program: Biotechnology

submitted to

**Graz University of Technology**

## **Supervisor**

Dr. Anita Emmerstorfer-Augustin

Dr. Simon Arhar

Univ.-Prof. Robert Kourist

Institute of Molecular Biotechnology

Graz, September 2024

**Affidavit**

I declare that I have authored this thesis independently, that I have not used other than the declared sources/resources, and that I have explicitly indicated all material which has been quoted either literally or by content from the sources used. The text document uploaded to TUGRAZonline is identical to the present master's thesis.

---

Date

---

Signature

## **Acknowledgements**

First and foremost, I want to thank my supervisor, Anita Emmerstorfer-Augustin, for her outstanding guidance throughout this project. Anita continuously provided new ideas and solutions, which were crucial in overcoming challenges we faced. I also want to thank Prof. Robert Kourist for taking on the official supervision of my work and thoroughly reviewing my thesis.

I am deeply grateful to Simon Arhar for his excellent support and mentorship during the entire process. He provided me with valuable insights into biotechnology, experimental planning and result interpretation. With never ending patience, he made this journey so enjoyable, and I greatly appreciate the learning experiences I had under his supervision.

Lastly, I want to thank the colleagues of the Emmerstorfer-Augustin research group, who created the best possible working environment. The sense of community we developed brought immense joy to my time on this project.

## Abstract English

*Cupriavidus necator* is gaining increasing attention in modern biotechnology due to its ability to grow on carbon dioxide, and its potential for producing bioplastic precursors and single-cell protein. Yet, genetic engineering of this organism has so far been challenging due to limited knowledge of its molecular biology and the lack of effective genome editing methods. This Master thesis presents the establishment of a lambda RED recombination system for use in *Cupriavidus necator* H16. In combination with electroporation of vector DNA, the recombineering system enables an efficient and fast gene deletion methodology utilizing suicide plasmids or, for the first time, linear PCR product. The novel lambda RED system was validated for the knockout of the three different loci (*eGFP*, *proC*, and *eda*) and, as a proof-of-concept, ultimately utilized for stable genomic integration of the *Escherichia coli* phytase gene *appA* into the *phaC1* locus of *C. necator*. A Cre/loxP system further enabled efficient marker recycling. The combination of a minimal transformation protocol with lambda RED recombineering and a Cre/loxP system offers a robust, freedom-to-operate synthetic biology tool in an alternative bacterial production host. This approach simplifies genome engineering in *C. necator* and is expected to significantly enhance future strain development efforts.

## Abstract Deutsch

*Cupriavidus necator* gewinnt derzeit massiv an Aufmerksamkeit in der modernen Biotechnologie aufgrund seiner Fähigkeit, auf Kohlendioxid zu wachsen, und seines Potentials zur Produktion von Biokunststoffen und Einzeller-Proteinen. Die genetische Manipulation dieses Organismus gestaltet sich bislang jedoch schwierig, da nur begrenztes Wissen über den Organismus vorhanden ist und effektive Methoden zur Genom-Editierung fehlen. Diese Masterarbeit beschreibt die Etablierung eines lambda RED-Rekombinationssystems für den Einsatz in *Cupriavidus necator* H16. In Kombination mit der Elektroporation von Vektor-DNA ermöglicht das Rekombinierungssystem eine effiziente und schnelle Methode zur Gen-Deletion, wobei sowohl Suizidplasmide als auch erstmals lineare PCR-Produkte verwendet werden. Das neuartige lambda RED Rekombinierungssystem wurde für den Knockout der drei unterschiedlichen Loci (*eGFP*, *proC*, und *eda*) validiert und als Proof-of-Concept letztlich für die stabile genomische Integration des Phytase-Gens *appA* von *Escherichia coli* in den *phaC1*-Locus von *C. necator* eingesetzt. Ein Cre/loxP-System ermöglichte zudem eine effiziente Markerexzision. Die Kombination eines minimalen Transformationsprotokolls mit dem lambda RED Rekombinierungssystem und einem Cre/loxP-System bietet ein robustes, frei nutzbares Werkzeug der synthetischen Biologie in einem alternativen bakteriellen Produktionswirt. Dieser Ansatz vereinfacht die Genom-Editierung in *C. necator* und wird voraussichtlich die zukünftigen Bemühungen zur Stammentwicklung erheblich verbessern.

## Table of contents

|   |    |
|---|----|
| Affidavit.....  | 2  |
| Acknowledgements .....  | 3  |
| Abstract English.....   | 4  |
| Abstract Deutsch.....   | 4  |
| Table of contents.....  | 5  |
| 1. Introduction .....   | 6  |
| 2. Results.....   | 8  |
| 2.1 Design of a recombineering system for gene knockouts in <i>C. necator</i> .....                             | 8  |
| 2.2 Efficient knockout of native <i>proC</i> and <i>eda</i> loci using suicide plasmids and linear fragments... | 12 |
| 2.3 Recombineering-based introduction of marker free phytase expression in <i>C. necator</i> .....              | 14 |
| 3. Discussion.....  | 18 |
| 4. Materials and Methods .....  | 21 |
| 4.1 Bacterial strains and cultivation conditions .....  | 21 |
| 4.2 Cloning and DNA delivery .....  | 21 |
| 4.3 Strain construction.....  | 22 |
| 4.4 Fast transformation of <i>C. necator</i> .....  | 22 |
| 4.5 Phytase activity assay .....  | 23 |
| 4.6 PHB staining .....  | 23 |
| 4.7 Plasmid loss .....  | 23 |
| 5. References.....  | 25 |
| 6. Supporting information.....  | 30 |
| 6.1 Loci targeted in this work.....   | 30 |
| 6.2 Plasmids used in this work.....   | 30 |
| 6.3 Cloning of plasmids used in this study .....  | 31 |
| 6.4 Additional data .....   | 37 |

## 1. Introduction

*Cupriavidus necator* H16, formerly known as *Ralstonia eutropha* H16, is a Gram-negative soil bacterium with a highly versatile metabolism. The genome of *C. necator* consists of two chromosomes and a megaplasmid, together encoding more than 6,000 annotated genes (1). Under autotrophic conditions, *C. necator* utilizes the Calvin-Benson-Bassham (CBB) cycle, enabling it to thrive on CO<sub>2</sub> as sole carbon source. The energy required for the carbon fixation is derived from the oxidation of hydrogen gas H<sub>2</sub>, carried out by oxygen-tolerant [NiFe]-hydrogenases (2). Under heterotrophic conditions, *C. necator* is able to metabolize a variety of organic compounds, including sugars, organic acids and amino acids (3). Sugars like fructose and N-acetyl glucosamine are metabolized via the Entner-Doudoroff pathway, an alternative to glycolysis, which is especially characterized by the intermediate ketodesoxyphosphogluconate and its cleavage by the aldolase Eda (4). Notably, *C. necator* has the ability to synthesize polyhydroxybutyrate (PHB), a biodegradable polyhydroxyalkanoate (PHA) that has gathered significant attention for its potential in bioplastics production. For instance, recent work has demonstrated that *C. necator* H16, when grown under autotrophic conditions, can accumulate PHB comprising up to 79% of its total biomass (5). It is therefore not surprising that PHA production in *C. necator* is of growing industrial interest, with ongoing efforts focusing on further optimizing this process. Metabolically, the accumulation of PHB in intracellular granules serves as a reserve for carbon and energy storage. One of the key biosynthetic enzymes in this process is the PHA synthase, which is encoded by *phaC1* and catalyzes the polymerization of the precursor 3-hydroxybutyryl-CoA into PHB. (recently reviewed in (6)) The use of strains with a defect *phaCAB* operon is frequently considered in metabolic engineering strategies, since the disruption of PHB synthesis redirects metabolite flux into other pathways leading to increased yields of alternative products (7–9)

Currently, the introduction of recombinant DNA for the genetic engineering of *C. necator* is predominantly accomplished via conjugation. First established by Simon et al. in 1983, traditional suicide plasmids still serve as the major method for classic modification of the *C. necator* genome by homologous recombination (10). This strategy involves cloning of the desired DNA into a mobile plasmid, transforming this plasmid into an *E. coli* S17-1 donor strain, and then facilitating the conjugative transfer of the plasmid into the recipient strain (11,12). Overall, conjugation is a labor-intensive and time-consuming method that often exhibits low efficiency, limiting its application in high throughput settings. As an alternative, electroporation has emerged as a more time-efficient method for introducing DNA into *C. necator*. Early protocols were functional but exhibited inconsistent transformation efficiencies, which were found to be heavily dependent on the construct being used (13,14). Recent advancements have addressed these limitations by improving the understanding of *C. necator*'s restriction modification system. Xiong et al. identified and deleted several restriction endonucleases in *C. necator*, leading to the development of a *H16-A0006* mutant strain, which demonstrated a 1600-fold increase in transformation efficiency (15). Recently, Vajente et al. identified the recognition sequence of *H16\_A0006* and the benefits of using unmethylated or natively methylated plasmids for electroporation into *C. necator*, by usage of an *E. coli dam/dcm* strain or re-extraction of plasmids from *C. necator* H16. Building on this knowledge, they successfully performed electroporation of a suicide plasmid for gene knockout. However, compared to a similar approach of using suicide plasmids for engineering *E. coli* in

the late 90s (16), which achieved electroporation rates of approximately  $1 \times 10^3$  cfu/ $\mu$ g DNA, the current method's rate of 8 cfu/ $\mu$ g DNA is more than 100 times lower. This significantly lower efficiency raises concerns about the suitability of this approach for more complex genetic engineering tasks. (17) Given that these recent results represent significant progress in the electroporation of *C. necator*, the next logical step would be to improve the recombination efficiency to further accelerated strain engineering. This could involve developing a robust tool based on this fast gene delivery methods, such as CRISPR/Cas9. However, while initial attempts to apply the CRISPR technology in *C. necator* have shown some promise, it has shown limited versatility and prolonged experimental durations (15).

To enhance native recombination systems, phage-derived recombineering methods offer powerful solutions (18). These methods are well-established in model organisms like *E. coli* and are used to introduce recombinant genes, perform knockouts, and insert point mutations, offering high efficiency and precision in genome modifications. Notably, they stand out as versatile and robust tools for genetic engineering, and unlike CRISPR/Cas9 strategies, they provide the advantage of a well-established freedom-to-operate framework. The lambda RED recombineering strategy has proven to be particularly successful (18,19) and works by enhancing homologous recombination through the additional expression of genes encoding an annealase/single-strand binding protein (Beta), an exonuclease (Exo), and an inhibitor of the bacterial host's recBCD system (Gam) (20). These genes are typically controlled by an inducible promoter on an easily curable, low-copy-number plasmid (21,22). The delivery system for the recombinant or mutated gene is usually provided on linear DNA fragments, or occasionally on circular plasmids. When circular plasmids are used, so-called suicide plasmids are often employed in an 'in-out' strategy, where the gene of interest on the plasmid is first recombined into the bacterial target locus, followed by resolution of the cointegrate (23). This method is frequently used with vectors that cannot replicate under the conditions used for cointegrate selection, or by using origins of replication with low stability (23). In cases where more stable plasmids are used, RED recombineering can also be applied to retrieve genes from the bacterial chromosome onto the plasmid backbone, such as by exchanging a selection marker flanked by 50-nt homologous regions with the target sequence (24). However, due to the genetic instability associated with the use of plasmids, the use of linear DNA fragments, typically generated by PCR amplification, is generally preferred in recombineering approaches (22).

The genes used in lambda RED recombineering derive from bacteriophage lambda, making the system particularly effective in *E. coli*. However, it has also been adapted for use in diverse alternative bacterial hosts, including *Vibrio cholerae* and *Pseudomonas aeruginosa* (reviewed by (18)). The extent to which the system needs modification depends on the phylogenetic distance of these bacteria from *E. coli*. In many cases, adaptations to the expression machinery are necessary to suit the host organism (25–27). In this context, we here report the development of a straightforward lambda RED recombineering system for use in *C. necator* by utilizing recently established low-copy-number plasmids (28). We demonstrate the system's effectiveness by successfully knocking out three different genes using either suicide plasmids or linear DNA fragments, achieving editing efficiencies above 64% and 74%, respectively. Additionally, we employed the lambda RED system for the stable integration of the *appA* gene, which encodes a phytase, into the *phaC1* locus. To further enhance this system, we implemented marker

recycling using the Cre/loxP system, encoded on an electroporation plasmid, to efficiently generate marker-free strains.

## **2. Results**

### **2.1 Design of a recombineering system for gene knockouts in *C. necator***

To establish recombineering in *C. necator*, a plasmid was constructed to express the lambda RED system (Fig. 1). The rhamnose promotor from *E. coli* was already reported to be tightly controllable in *C. necator* (29,30) and, therefore, utilized to enable rhamnose-induced gene expression of the three lambda RED genes. Additionally, a previously published ribosome binding site for *C. necator* (7) was used for polycistronic expression of the phage genes. The plasmid also incorporates the low copy number pSa origin of replication (28) and a tetracycline resistance cassette for plasmid maintenance. Lambda Exo, Gam and Beta production was induced during preparation of electrocompetent cells, as is standard in other bacterial systems (31). The model strain used in this study contained an *eGFP* expression cassette integrated into the *phaC1* locus for easy detection of successful integration events. Notable growth defects were observed with prolonged induction times of the lambda RED system. Thus, rhamnose was added only during the final cell density doubling before harvest to minimize the risk for unwanted background mutations, as observed in *E. coli* K-12 (32). Double-stranded DNA vectors for recombineering were designed to replace the genomic *eGFP* cassette in the model strain with a kanamycin resistance cassette through homologous recombination (Fig. 1). The knockout cassettes were introduced either via suicide plasmid with the relatively unstable pLO3 origin of replication (33), or as PCR product containing the resistance cassette and homologous regions corresponding to the target locus.



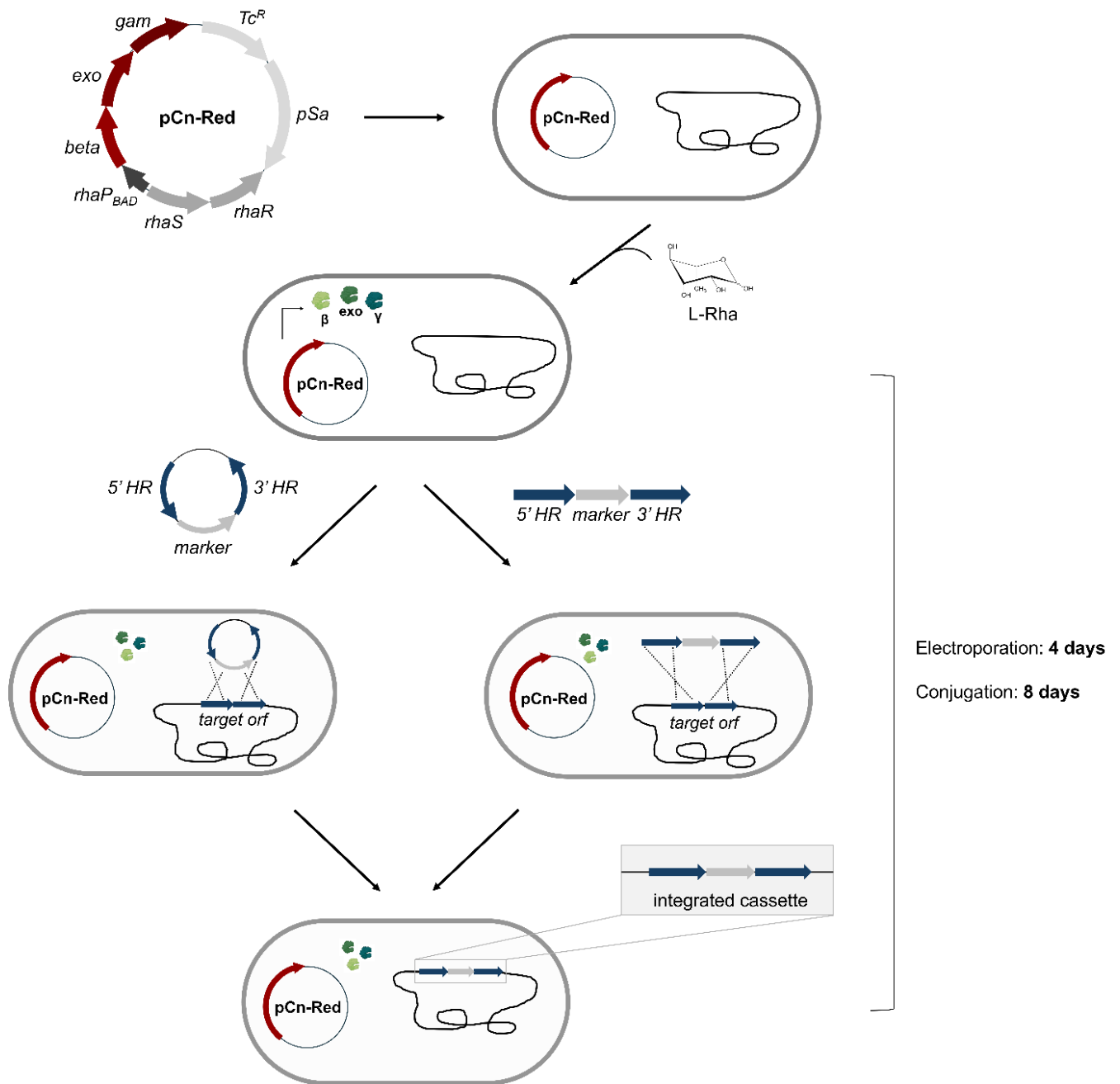


**Figure 1: Schematic overview of the lambda RED recombineering system adapted for *C. necator*, utilized for targeted locus replacement.** *C. necator* H16 cells are transformed with a plasmid that expresses lambda Beta, Exo and Gam, with induction achieved through rhamnose. The strain, producing lambda RED, is then transformed with either a suicide plasmid or linear fragment, both containing the marker flanked by sequences homologous to the target locus in the genome. Lambda RED facilitates the replacement of the target locus with the marker cassette through double crossover. Electroporation of the constructs enables immediate transformation and subsequent recombination events, proving to be twice as fast as traditional conjugation methods.

Cells transformed with circular and linear fragments were screened for the recombination events by plating on kanamycin-containing agar plates and checking for the loss of fluorescence (Fig. 2, A and B). For the suicide plasmid, the use of the heterologous recombineering system increased transformation rates from approximately 12 cfu/ $\mu$ g DNA to  $4.8 \times 10^2$  cfu/ $\mu$ g DNA (Fig. 2, C). No transformants were

observed with the linear PCR product in cells not expressing lambda RED. However, in cells expressing lambda RED, approximately  $2.2 \times 10^2$  cfu/ $\mu$ g DNA were achieved. These data, obtained from three technical and two biological replicates of competent cells separately prepared in two different batches, highlight significant batch-to-batch variation and account for the high standard deviation observed (Fig. 2, C). Editing efficiencies were calculated (Fig. 2, D) based on the analysis of 50 clones per electroporation and whether or not they exhibited fluorescence under UV light (Fig. 2, E). Independent of the presence of lambda RED, an editing efficiency of around 64% was found with the suicide plasmids (Fig. 2, D). The linear fragment transformed into the strain expressing lambda RED exhibited an editing efficiency of 90%. To verify the correlation between phenotype and genotype, 10 clones per transformation showing the expected phenotype were analyzed by colony PCR. All clones tested by colony PCR exhibited the correct 3 kb PCR product, confirming successful replacement of the target locus with the *kanR* cassette (Fig. 2, F).

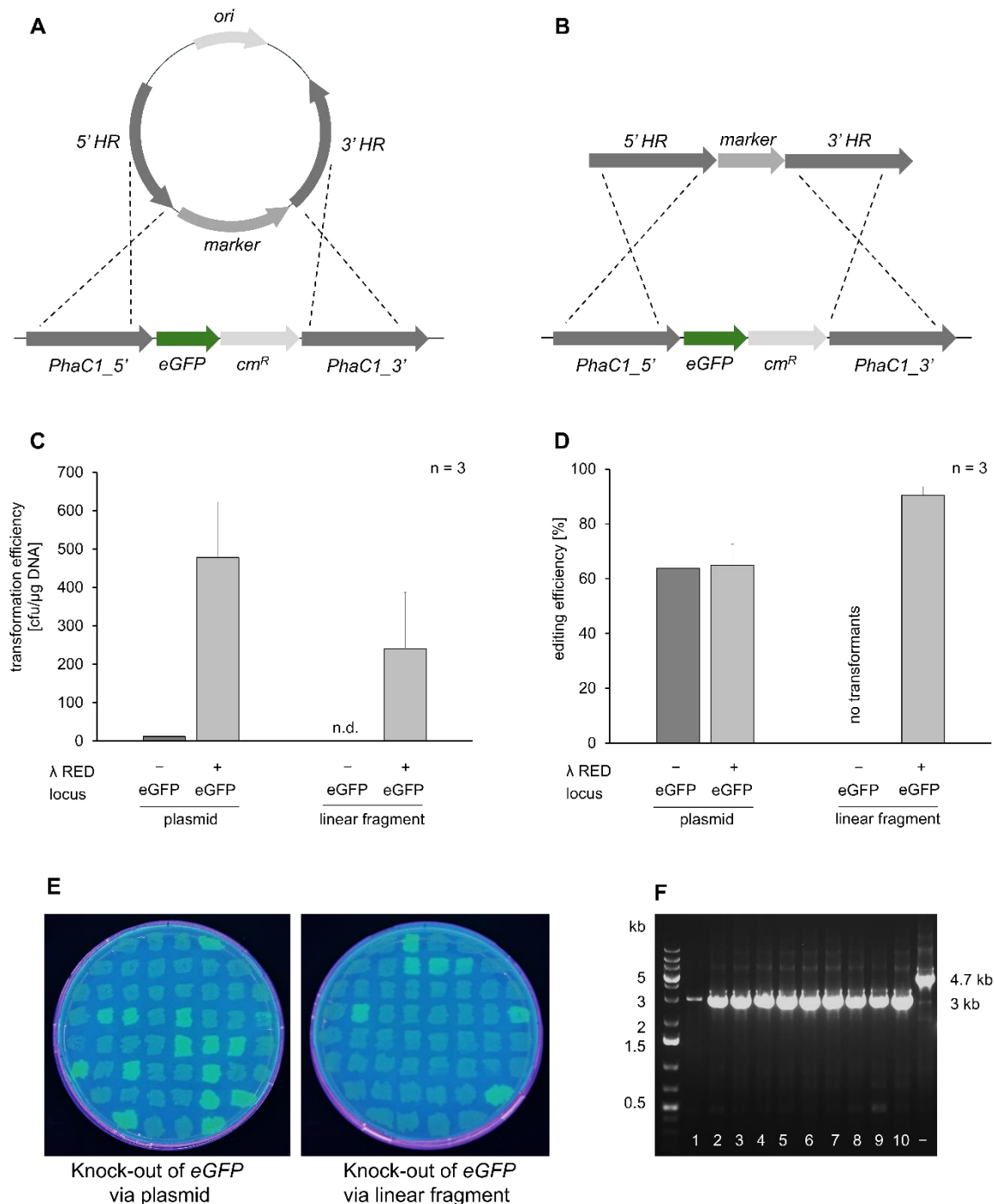


**Figure 2: Suicide plasmid and linear PCR product derived vectors efficiently replaced genomic *eGFP* through lambda RED-aided recombination.** (A) Schematic representation of a suicide plasmid designed for targeting the *eGFP* locus. The integration cassette includes a selection marker flanked by homologous sequences, with the expected sites of a double crossover indicated. (B) Schematic of a linear double-stranded DNA, generated by PCR, targeting the locus. This fragment mirrors the integration cassette of the suicide plasmid. (C) Transformation efficiencies for the *eGFP*-targeting suicide plasmid and the PCR product were calculated for cells with and without expression of the lambda RED system. Data from three transformations using two separate batches of electrocompetent *C. necator* cells show no transformants for the linear DNA in cells lacking the lambda RED system. (D) Editing efficiencies of each construct targeting *eGFP* were determined based on fluorescent phenotypic screening of 50 colonies per transformation. (E) Example of phenotypic screening: Transformants that lost fluorescence, indicating a positive recombination event at the *eGFP* locus, are shown for the suicide plasmid (left) and PCR-derived vector DNA (right). (F) Verification of the correlation between phenotype and genotype was conducted via colony PCR for 10 clones per transformation. The *eGFP* locus (-) produced a 4.7 kb PCR product, while replacement with the *kanR* cassette yielded a 3 kb PCR product.

## 2.2 Efficient knockout of native *proC* and *eda* loci using suicide plasmids and linear fragments

After establishing a proof of principle for the recombineering system with the *eGFP* locus, the approach was further validated by targeting the native *C. necator* loci of *proC* and *eda*, which code for a pyrroline-5-carboxylate reductase and a keto-desoxy-phosphogluconate aldolase, respectively. Knockout of *proC* results in proline dependency, whereas knockout of *eda* impairs growth on sugars due to its role in the Entner-Doudoroff pathway, producing easily detectable phenotypes (34,35).

*C. necator* H16 cells expressing the lambda RED system were transformed with suicide plasmids and linear fragments designed to target the two loci via homologous recombination. Targeting the *proC* locus, the transformation rates were around  $2 \times 10^2$  cfu/ $\mu$ g DNA for the suicide plasmid and 9 cfu/ $\mu$ g DNA for the linear PCR product (Fig. 3, A). Putative  $\Delta$ *proC* mutants were identified by screening transformants on minimal agar plates with and without 0.2 % proline. Clones that grew only on proline-supplemented agar plates were considered recombinant and used for the calculation of editing efficiencies (Fig. 3, B and C). The suicide plasmid yielded an editing efficiency of around 96 %, while the linear fragment yielded 92 % (Fig. 3, B). Again, the correlation between phenotype and genotype was verified by analyzing 10 clones exhibiting the correct phenotype through colony PCR. Primers were designed to produce a PCR product only if the *kanR* cassette was correctly integrated at the locus (Fig. 3, D). Similarly, cells transformed with constructs targeting *eda* were selected on kanamycin agar containing 2% lactate as an alternative carbon source to fructose. The transformation rate for the suicide plasmid was again approximately  $2 \times 10^2$  cfu/ $\mu$ g DNA, while the linear fragment achieved 25 cfu/ $\mu$ g DNA (Fig. 3, A). To identify potential  $\Delta$ *eda* mutants, the transformants were selected on minimal medium containing 2 % fructose or 2 % lactate. Clones growing exclusively on lactate-containing medium were considered *eda* knockout candidates (Fig. 3, E). The suicide plasmid achieved an editing efficiency of around 89 %, while the linear fragment yielded 74 % (Fig. 3, B). Genotype verification was performed by colony PCR, with a 500 bp shift of the amplicon expected upon replacement of *eda* by the kanamycin resistance cassette.

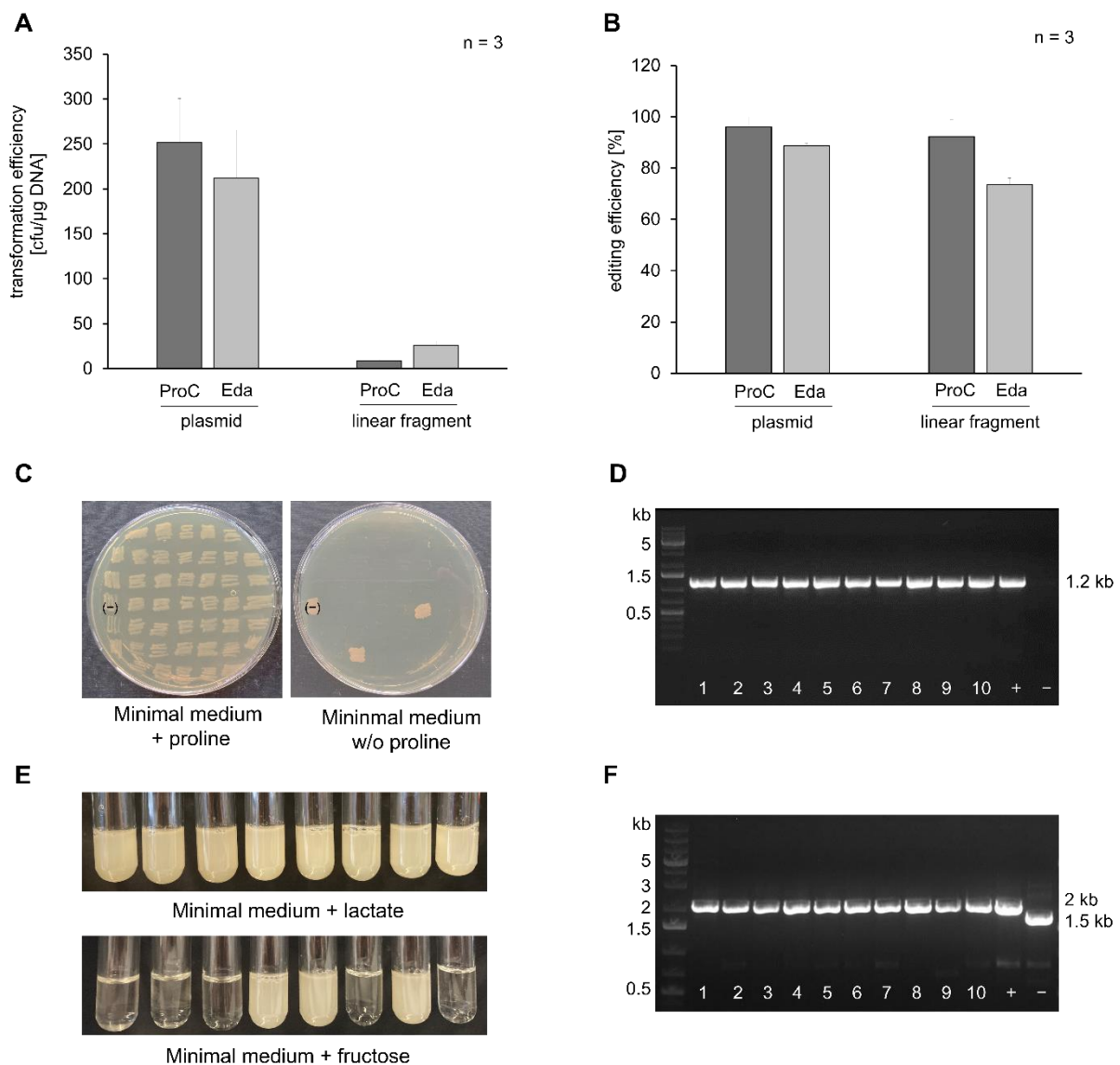


**Figure 3: Native loci *proC* and *eda* were efficiently replaced using both suicide plasmid and linear DNA vectors through lambda RED-aided recombineering.** (A) Transformation rates for suicide plasmids and linear vector DNA targeting *proC* and *eda* were evaluated. (B) Editing efficiencies for these constructs were calculated. (C) For phenotypic screening, transformants were restreaked on minimal medium with (left) and without proline (right). Clones that grew exclusively on medium supplemented with proline were identified positive for a replacement of the *proC* locus. (D) Genotypic verification of  $\Delta proC$  phenotype via PCR. The wildtype *proC* locus (-) showed no PCR product with the selected primers, whereas the integrated *kanR* cassette resulted in a 1.2 kb PCR product. (E)  $\Delta eda$  mutants were identified by comparing growth on minimal medium with lactate (top) and versus minimal medium with fructose (bottom). Transformants that grew only on lactate were considered potential  $\Delta eda$  mutants. (F) Genotypic verification of  $\Delta eda$  mutants was conducted via PCR. The wild-type *eda* locus (-) produced a 1.5 kb PCR product, while the integrated *kanR* cassette yielded a 2 kb PCR product.

### 2.3 Recombineering-based introduction of marker free phytase expression in *C. necator*

To broaden the application of the lambda RED recombineering system, the integration of the *E. coli* *appA* gene, which encodes a phytase, into the *C. necator* genome was investigated. Two strains were utilized: the wild-type H16 and the *eGFP* strain, which has an *eGFP* expression cassette integrated into the *phaC1* locus. The integration module was designed to contain an *appA* expression cassette with a kanamycin resistance marker flanked by loxP sites, and two homologous regions up- and downstream of the whole cassette for recombination into the *phaC1* locus (Fig. 4).

When targeting the *phaC1* or *eGFP* locus with the suicide plasmid harboring *appA*, an interesting observation was made. Amplification of the DNA inserted between the two homologous arms on the plasmid revealed PCR products of varying sizes, which matched both the initial *appA* expression cassette, but also the size of the wild-type and *eGFP* locus targeted to be replaced in the genome (Fig. S1). Cells did not eliminate the plasmid as expected but instead stably maintained it for an extended period, as determined by colony PCR (Fig. S2). Although plasmid isolation and sequencing did unfortunately not produce analyzable results, these findings raised concerns. When using stable plasmids, recombineering can be employed to retrieve genes from bacterial chromosomes (24). This raises the possibility that with an active lambda RED system present, there could be recombination events leading to genetic instability, with the target and recombinant genes potentially switching between the two different genomic loci. Consequently, we decided to exclusively use linear PCR products for *appA* integration. Transformation rates varied depending on whether the wild-type or *eGFP* strain was used, with approximately 7 cfu/μg for the wild-type strain and 30 cfu/μg for the *eGFP* strain (Fig. 4, A). Colonies from both *C. necator* strains were analyzed for successful *appA* integration via colony PCR (Fig. S3 – S5). The editing efficiency for the linear fragment targeting *phaC1* was approximately 87%, nearly three times higher than the 30% editing efficiency observed for the *eGFP* locus (Fig. 4, B).

To recycle the kanamycin resistance marker co-integrated with the *appA* expression cassette, a small plasmid encoding the Cre recombinase under the control of a cumate-inducible tac promoter was designed. This plasmid was transformed into readily engineered *C. necator* strains using a minimal transformation protocol (36) to streamline the preparation of competent cells (Fig. 4, C). Transformants were selected on chloramphenicol plates containing *p*-cumate. To identify those that had lost the antibiotic resistance marker, transformants were restreaked on plates with and without kanamycin (Fig. 4, D). All tested clones exhibited a loss of kanamycin resistance after two rounds of the procedure. Correct marker recycling was confirmed for all tested clones using colony PCR (Fig. 4, E).

To ensure the removal of the pCn-Red plasmid, which expresses the lambda RED system in *C. necator* H16, a protocol for plasmid curing was implemented. The *C. necator* cells were incubated in minimal medium for 48 h over two incubation cycles, allowing adequate time for natural plasmid loss. Following this period, the cells were streaked onto agar plates with and without tetracycline. None of the clones grew on tetracycline-containing plates, confirming the successful loss of the plasmid in all restreaked clones. The pCn-Cre plasmid for expression of the site-specific recombinase was easily lost by the same plasmid curing steps, given the plasmid's unstable origin of replication.

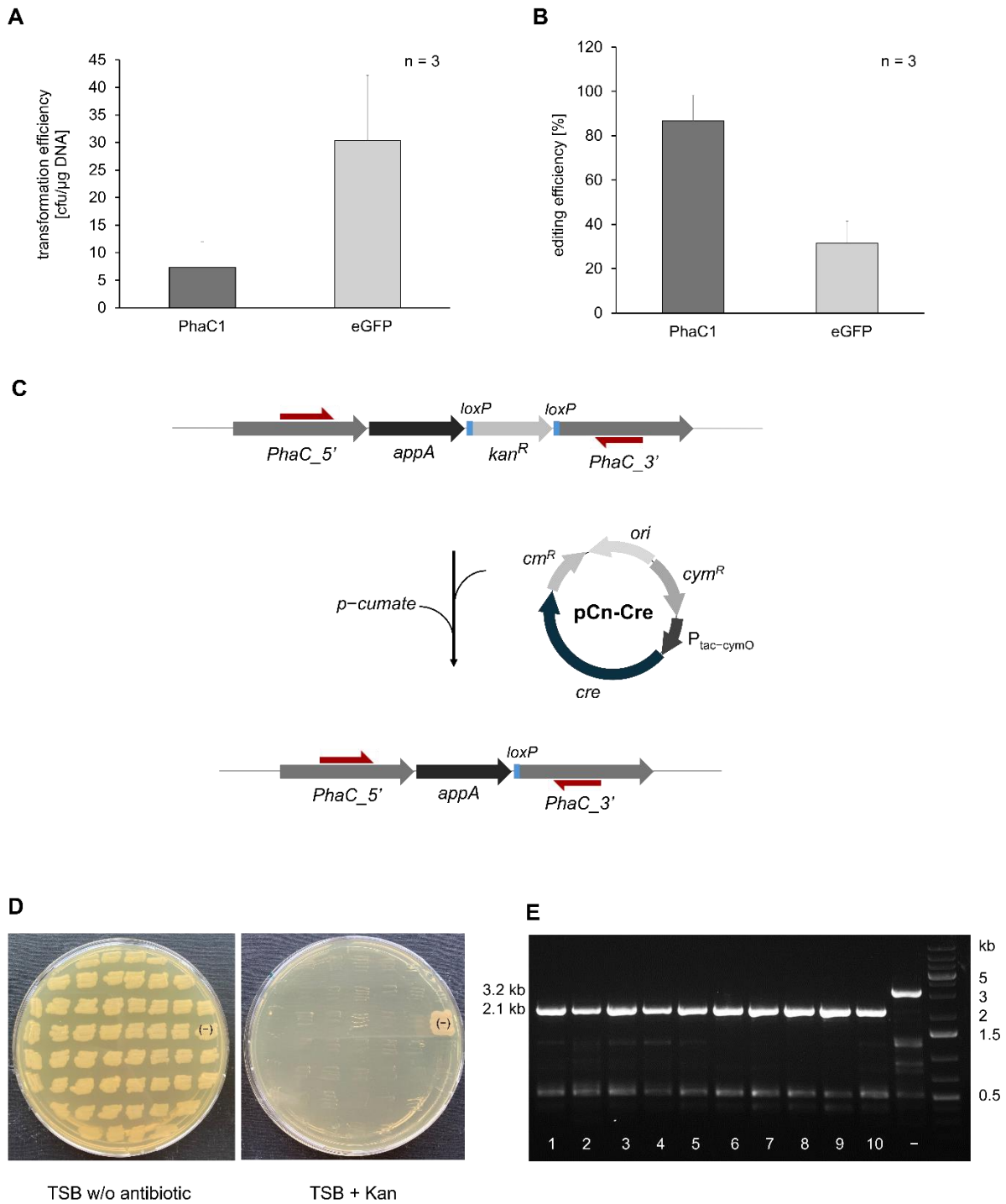


**Figure 4: The *appA* expression cassette is integrated into the *phaC1* locus with subsequent marker recycling using the Cre-lox recombination system.** (A) Transformation rates and (B) editing efficiencies of the *appA* cassette integrated into the *phaC1* locus of *C. necator* wild-type and the *eGFP* expression strain are shown. (C) A schematic of marker recycling using the Cre-lox recombination system, with the Cre recombinase encoded on the pCn-Cre plasmid and controlled by a cumate inducible promoter, is provided. (D) Screening for marker free mutants was conducted by restreaking on agar plates with and without kanamycin. Transformants that grew only on TSB without antibiotics were considered marker-free. (E) Genotypic verification of marker recycling was performed via colony PCR. Before marker recycling, a PCR product of 3.2 kb was expected. Successful removal of the *kanR* cassette resulted in a 2.1 kb PCR product.

A marker free *C. necator* strain with the *appA* cassette integrated at the *phaC1* locus, confirmed via colony PCR, was further analyzed for its PHB content and phytase activity. The *phaC1* gene encodes the key enzyme responsible for catalyzing the polymerization of hydroxyacyl-CoA monomers into the PHB polymers. Consequently, the disruption of *phaC1* by the *appA* expression cassette was expected to eliminate PHB production. To visualize the loss of PHB granules in the phytase expression strain, PHB staining with Nile red followed by fluorescence microscopy was performed (Fig. 5, A). *C. necator* H16 wild-type and the PHB negative PHB<sup>-4</sup> (37) strains were used as controls. As expected, the wild-type *C. necator* H16 strain accumulated significant PHB granules, indicated by intracellular fluorescence signals under the tested cultivation conditions (Fig. 5, B). In contrast, both the PHB-negative PHB<sup>-4</sup> strain and the marker-free *appA* expression strain showed no detectable signals during fluorescence microscopy. Phytase activity in the strain was evaluated by measuring phosphate release from phytic acid incubated with cell lysate. The newly developed *appA* expression strain was compared with wild-type *C. necator* H16 and an episomal *appA* expressing strain previously generated in our lab (28). Incubation of phytic acid with our marker-free genomic *appA* expression strain resulted in the release of approximately 8  $\mu\text{mol}$  of phosphate per OD<sub>600</sub> unit over a 15 min reaction period. In comparison, the strain expressing *appA* from the high-copy-number, pKPrepPar\_Pj5 plasmid released around 15  $\mu\text{mol}$  of phosphate per OD<sub>600</sub> unit (Fig. 5, B). These data were obtained from three biological and two technical replicates.



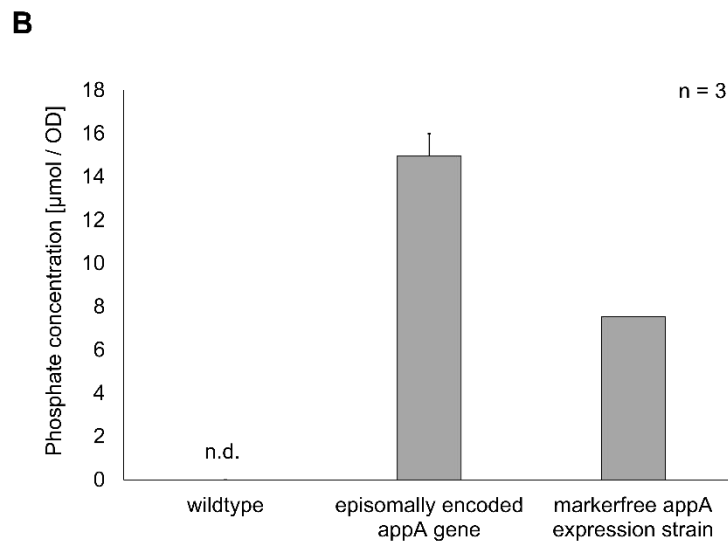
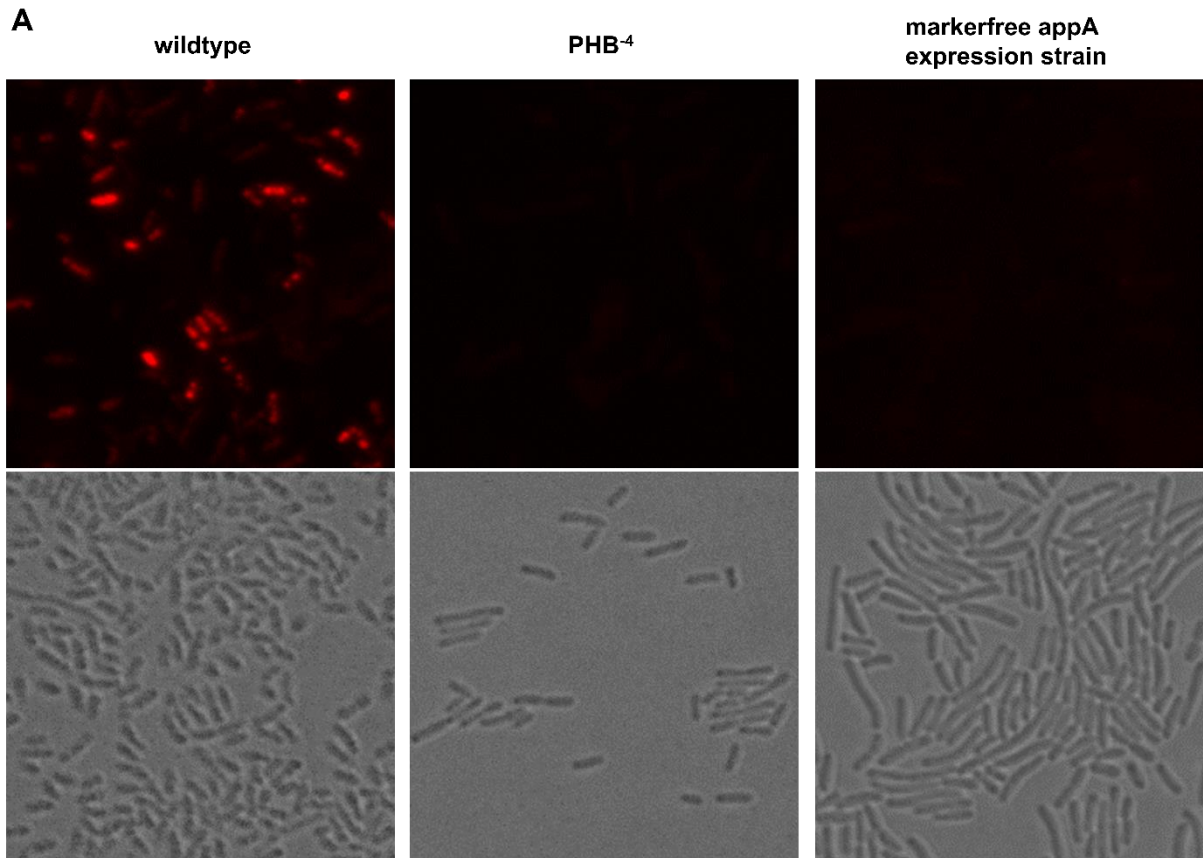


**Figure 5: Investigation of a marker-free *appA* expression strain was conducted to assess its PHB phenotype and phytase activity.** (A) The disruption of *phaC1* by *appA* was verified by Nile Red staining and subsequent fluorescence microscopy. The marker-free *appA* expression strain is compared with *C. necator* H16 wild-type and *C. necator* PHB<sup>-4</sup>. Each image represents a 25.5 x 25.5 μm section. (B) Phytase activities were evaluated by measuring the phosphate released from phytic acid after 15 min of incubation with cell free lysate of the strains. Lysates from *C. necator* wild-type and a strain expressing *appA* episomally were used as controls.

### 3. Discussion

Lambda RED recombineering was initially developed for *E. coli*, utilizing the native lambda phage open reading frame for the *beta*, *exo*, and *gam* genes (38). While this system has been successfully adapted for genetic manipulation in bacteria closely related to *E. coli*, such as the Gamma-proteobacteria *Salmonella enterica* (39,40) and *Klebsiella pneumoniae* (41,42), its functional range is more limited in other bacterial species, particularly for dsDNA recombination. For instance, its application in Beta-proteobacteria, to which *C. necator* belongs, has been rarely reported (reviewed by (19)), and often requires more advanced modifications, as for example the introduction of alternative annealases (43,44). Further, a lambda infection of *C. necator* has to the best of our knowledge, not been reported yet, suggesting a direct application of lambda RED recombineering may be challenging. In the lambda phage, the original *beta* and *exo* open reading frames overlap, and we hypothesized that this may complicate polycistronic expression in non-model bacteria like *C. necator*. To mitigate potential issues with polycistronic DNA expression, ensure full expression, and prevent read-through expression of the ORF, we thus placed *C. necator* ribosome binding sites (7) upstream of each RED gene. Since expression levels typically decrease for downstream genes in a polycistronic operon (45), we also reordered the genes to *beta*, *exo* and *gam*, based on their importance in the recombineering process. Beta, the annealase directly responsible for recombination, was placed first. Gam, which is not directly involved in recombination and lacks a clear target in *C. necator* due to the absence of a RecBCD system (46), was placed last. It has been reported multiple times that prolonged exposure to lambda RED recombineering can lead to unwanted background mutations or growth defects (32). To minimize these risks, most plasmid-encoded recombineering systems are controlled by tightly regulatable promoters, such as the arabinose promoter, which is known for its inducible, high-level expression (21,22,47). In *C. necator*, the rhamnose-inducible promoter has been reported to offer even tighter regulation than the arabinose promoter (29,30), which is why we used it for lambda RED expression. As demonstrated in this study, these strategies specifically designed for Beta, Exo and Gam production were sufficient to achieve efficient recombineering in *C. necator*.

We initially assessed the effectiveness of the lambda RED system by targeting an *eGFP* cassette inserted into the *phaC1* gene, which provided a robust fluorescence-based readout for recombination success. The results demonstrated that the RED system not only facilitated gene replacement through its native recombination mechanisms but also achieved a 40-fold increase in transformation rates compared to transformants not expressing lambda RED. (Fig. 2, C). While the enhanced transformation efficiencies initially surprised us, we realized that using low-stability plasmids as gene delivery vehicles allowed for immediate integration of the selection marker into the target locus, which appears advantageous under selection pressure. However, we also observed potential stability issues associated with the plasmid: The *appA* suicide plasmid could still be fully amplified by colony PCR days after electroporation into the lambda RED producing strain (Fig. S1, S2). Our suicide plasmids were intentionally designed with the origin of replication from pLO3. The pLO3 origin, a ColE-type origin derived from pBR322, is prevalent in Enterobacterales and other Gamma-proteobacteria (48), but has been discussed as being incapable of autonomous replication in *C. necator* (49). ColE-type origins are also widely used in suicide plasmids for *C. necator* (15,33,50,51). However, to our knowledge, these

publications lack data on the half-life of these plasmids post-transformation. This fact and the observation that our own suicide plasmid does not disappear even after successful recombineering raises concerns about whether plasmid curing is consistently and fully achieved. In contrast to suicide plasmids, efficient integration of linear DNA in all three cases (*eGFP*, *proC* and *eda*) was fully dependent on the recombineering system. Although transformation rates were lower, they were at least as effective as those achieved with the corresponding suicide plasmids. Linear vector DNA offers the advantage of being easily generated through overlap extension PCR, eliminating the need for *E. coli*-based plasmid assembly. Additionally, PCR products are not methylated, reducing the risk of restriction endonuclease-mediated electroporation issues (17). Since linear DNA fragments are typically degraded quickly by bacterial exonucleases, they cannot be maintained in *C. necator* without genomic integration, which helps minimize the stability issues observed with suicide plasmids.

As a proof of concept, we integrated an *appA* expression cassette via electroporation of a PCR product into the *phaC1* locus of wild type *C. necator* and our *eGFP* expression strain. The *appA* gene encodes for a bacterial phytase that breaks down phytate (IP6) into lower inositol phosphate forms (IP5-IP1) and inorganic phosphate (52). As phytases provide the main source of phosphate for monogastric animals, they are considered an important feedstock supplement (53). We recently published the production of AppA from highly stable episomal plasmids in *C. necator* (28). Although these plasmids are stably maintained in the expression host without any antibiotic selection pressure, they still carry the antibiotic resistance gene necessary for electroporation. In industrial applications, the presence of an antibiotic resistance gene is often undesirable. To address this, we utilized the Cre/loxP site-specific recombinase system, a preferred method for removing genomically integrated marker cassettes (3). By applying a quick protocol for preparing competent cells, our marker recycling method became both fast and efficient, achieving efficiency rates of 90-100%. The analysis of phytase activity in our marker-free production strain, which harbors only one copy of *appA*, was unexpectedly high, reaching 50% of the activity observed in an episomal system using a pBBR1-based plasmid, which likely contains 7-40 copies of the gene (51,54). Nile red staining and fluorescence microscopy of the *appA* expression strain confirmed the anticipated depletion of PHB due to the disruption of the *phaC1* locus. While PHB is of interest as a precursor for degradable bioplastics, it cannot be digested by most animals and is therefore undesired in single-cell protein production.

One of the main advantages of our newly developed genome editing method is the short time required between gene delivery and obtaining the final engineered strains. If competent cells, which can be stored at -80°C, are already prepared, it takes only two days to obtain the target strains. In contrast, using conjugational suicide plasmids for the same purpose typically takes twice as long due to the need for fresh cultures and the mating of *C. necator* with the donor *E. coli* S17-1 strain. This timeframe does not take into account for the two rounds of restreaking often recommended to avoid transconjugant contamination with the donor strain (12). Another efficient method for electroporation-based genome engineering in *C. necator* is CRISPR/Cas9. However, this method requires a 144–168 hour induction with arabinose to achieve editing efficiencies comparable to our recombineering approach (15). Also, the current CRISPR/Cas9 method only allows for gene deletions, but does not provide a strategy for (marker-free) targeted insertion of recombinant DNA. In contrast, our lambda RED recombineering

approach provides a quicker and more versatile alternative. Furthermore, the licensing complexities associated with CRISPR/Cas9 make freedom-to-operate methods, such as the one described in this study, a more attractive choice.

In summary, our adapted lambda RED system recombineering offers a reliable and powerful tool for genome editing in *C. necator*. It enables efficient deletions and insertions, significantly reducing the time required for genome editing compared to the traditional conjugation methods and published CRISPR/Cas9 systems. The introduction of cassettes via electroporation further accelerates the process and minimizing the risk for genetic instability. Additionally, efficient marker recycling facilitates complex genome engineering, which is especially relevant in a bacterial host with significant potential in modern biotechnology.

## 4. Materials and Methods

### 4.1 Bacterial strains and cultivation conditions

*E. coli* TOP10 (Invitrogen) was used for cloning and plasmid propagation. *C. necator* H16 (DSM 428) was used for the knock-out studies. *C. necator* H16 PHB<sup>-4</sup> (DSM 541) was used for PHB staining and fluorescence microscopy.

*E. coli* was cultured at 37 °C in lysogeny broth (LB) medium, supplemented with either kanamycin [50 µg/mL], chloramphenicol [35 µg/mL] or tetracycline [12.5 µg/mL] depending on the antibiotic required for the respective cloning strategy. *C. necator* H16 was propagated at 28 °C in tryptic soy broth (TSB) medium supplemented with either gentamicin [20 µg/mL], chloramphenicol [75 µg/mL], kanamycin [200 µg/mL] or tetracycline [10 µg/mL] depending on the application. For screening specific locus knockouts, *C. necator* H16 clones were selected on minimal medium (MM) agar, prepared as described by Lambauer et al. (5), with 0.2 % proline or 2% lactate instead of fructose, depending on the respective knock-out strategy. Agar was added to a final concentration of 2 % for LB, TSB and minimal medium agar plates.

The transformation efficiency was measured as colony-forming units (CFU) per microgram of DNA. The editing efficiency was calculated as the ratio of transformants carrying the desired mutation to the total number of screened transformants. Each transformation was performed in biological triplicates, and the efficiency for each construct was determined. Transformants were initially screened based on phenotype, as detailed in the results section. Following phenotypic confirmation, genotypic validation was performed via colony PCR with primers designed to differentiate correct mutants from wild-type or off-target mutants by amplicon size. Editing efficiency was then calculated by dividing the number of correct mutants by the total number of screened transformants. For each transformation, 10 clones exhibiting the expected phenotype were selected for genotypical verification via colony PCR.

### 4.2 Cloning and DNA delivery

Targeted loci are specified in Supplementary Table S1 and all plasmids used in this work are listed in Supplementary Table S2. Plasmids were constructed via Gibson Assembly (55), and the exact cloning steps are described in the Supplementary information. Correct plasmid sizes were verified by restriction digestion analysis, and sequence confirmation was achieved by Sanger sequencing. Linear fragments were produced either by overlap extension PCR of individual DNA segments or by PCR amplification using suicide plasmids as templates. PCRs were performed using the Q5<sup>®</sup> High-Fidelity DNA Polymerase (New England Biolabs, Massachusetts, USA) following the manufacturers recommended protocol. PCR products for transformation of *C. necator* were purified via agarose gel electrophoresis. Native *C. necator* genes were amplified from genomic DNA of *C. necator*. For gel electrophoresis, the GeneRuler™ 1 kb Plus DNA ladder was used as a size standard. A detailed list of all primers and templates is provided in the Supplementary information (Table S3 – S11).

Electro-competent *C. necator* cells were prepared following the protocol from Taghavi et al. with slight modifications (14,28). Briefly, *C. necator* H16 strains were streaked on a TSB agar plate with the appropriate antibiotic and incubated at 28 °C for 48 h. A single colony was used to inoculate an overnight

culture supplemented with the same antibiotic and grown at 28 °C overnight. A main culture of 200 mL SOB medium (5 g/l yeast extract, 20 g/l tryptone, 0.6 g/l NaCl, 0.2 g/l KCl) was started at an OD<sub>600</sub> of 0.05 and incubated in 1 L unbaffled shake flasks at 28 °C. Once an OD<sub>600</sub> of 0.6 – 0.8 was reached, the culture was chilled on ice for 30 min and then transferred to eight 25 mL tubes. The cells were harvested by centrifugation at 4 000 rpm for 10 min at 4 °C. Each pellet was resuspended in 50 mL of 15 % (w/v) glycerol and centrifuged at 4 000 rpm for 10 min at 4 °C. This wash was repeated with 30 mL of 15 % (w/v) glycerol. A final wash was performed by resuspending the pellet in 5 mL glycerol and combining the eight pellets into four equal volumes. The cell suspensions were centrifuged at 4 000 rpm for 10 min at 4 °C. For each 0.1 OD<sub>600</sub> unit, 75 µL of 15 % (w/v) glycerol was added to the pellet and resuspended. Aliquots of 50 µL were shock-frozen in liquid nitrogen and stored at -80 °C.

Electroporation of *C. necator* H16 was performed using a MicroPulser™ electroporator (Bio-Rad, USA) with prechilled 2 mm electroporation cuvettes at 2.5 kV/cm. Plasmids (300 ng) and linear DNA fragments (1000 – 1500 ng, gel purified) were used for transformation. The shocked cells were allowed to recover in 1 mL SOC medium (20 g/l tryptone, 5 g/l yeast extract, 0.58 g/l NaCl, 2 g/l MgCl<sub>2</sub> • 6H<sub>2</sub>O, 0.186 g/l KCl, 2.46 g/l MgSO<sub>4</sub> • 7H<sub>2</sub>O, 3.96 g/l glucose-monohydrate) at 28 °C for 2 h before being plated on TSB agar with the appropriate antibiotics. The plates were incubated at 28 °C for 2 – 3 days.

#### **4.3 Strain construction**

The *C. necator* eGFP expression strain was created by modifying the previously published plnt\_lacY\_phaC\_loxP plasmid (50). In this modified plasmid, the *lacY* expression cassette was replaced with an eGFP controlled by a constitutive T5 promotor. Conjugation, using the *E. coli* S17-1 strain as a donor, was employed to introduce the plasmid into *C. necator* H16. Overnight cultures of *E. coli* S17-1 and *C. necator* H16 were diluted back to an optical density of 0.1 and 0.3, respectively. After 4h of incubation, five and seven OD<sub>600</sub>-units of each culture were harvested, resuspended in 600 µL of 0.9% sodium chloride solution, and combined. After a brief centrifugation at 1000 rpm for 30 s, the pellet consisting of *E. coli* S17-1 and *C. necator* H16 cells was resuspended in 100 µL sodium chloride solution, spotted on a TSB plate without antibiotics, and incubated overnight. After incubation, the spots were scraped off, resuspended in 1 mL of 0.9% sodium chloride solution, and plated in appropriate dilutions (typically undiluted-10<sup>-3</sup>) on TSB agar. Selection for genomic integration of the eGFP expression cassette into the *phaC1* locus was achieved with 100 µg/mL chloramphenicol, while 20 µg/mL gentamicin was used to eliminate *E. coli* contaminations. Colonies appearing after 2 days of incubation were restreaked twice to obtain pure *C. necator* strains.

#### **4.4 Fast transformation of *C. necator***

For iterative transformations of *C. necator*, a streamlined protocol was adapted (36) to eliminate the need for preparing electrocompetent *C. necator* cells, with the above-mentioned protocol, for each new transformation cycle. Each transformation starts by streaking the relevant strain onto a TSB agar plate with the appropriate antibiotic and incubating for 2 days at 28 °C. 10 mL SOB medium supplemented with antibiotic is then inoculated with a single colony and incubated overnight at 28 °C. The following day, a main culture of 20 mL SOB medium per transformation is inoculated to an OD<sub>600</sub> of 0.1 and grown at 28 °C until an OD<sub>600</sub> of 0.6 is reached. The cultures are then harvested by centrifugation at 4 000 rpm

for 5 min at 4 °C. The cell pellets are washed twice with 20 mL ice cold 0.2 M sucrose and after a final centrifugation, resuspended in 50 µL ice-cold 0.2 M sucrose. The cells are ready for immediate transformation using the described electroporation protocol.

#### **4.5 Phytase activity assay**

For the enzymatic phytate hydrolysis reaction, cell free extract of *C. necator* cells was prepared using the standard BugBuster protocol (Novagen, Merck). The BugBuster reagent was diluted 1:10 in Tris/HCl buffer (100 mM, pH 8) before use. The reaction was conducted in acetate buffer (100 mM, pH 4.5). Following the method of Arhar et al. (28), the cell-free extract was diluted 1:2 with acetate buffer before starting the reaction. The diluted CFE was mixed with acetate buffer and 80 mM sodium phytate to reach an end concentration of 8 mM sodium phytate in a final reaction mixture of 0.5 mL. The reaction occurred at 37 °C with gentle shaking. At 0 minutes (t<sub>0</sub>) and 15 minutes (t<sub>15</sub>), reaction samples were taken, stopped with 3 M HCl, and analyzed for phosphate release using the Saheki Method (56). For this, each reaction mixture was transferred to a 96-well plate and Saheki solution (12 mM ammonium molybdate, 80 mM zinc acetate and 2% ascorbic acid, pH 5) was added. After 15 min at room temperature, the samples were measured at 850 nm using the Eon High Performance Microplate Spectrophotometer (BioTek Instruments, Inc). KH<sub>2</sub>PO<sub>4</sub> standards were used for phosphate quantification. All measurements were performed in biological triplicates and technical duplicates.

#### **4.6 PHB staining**

The Nile Red staining of *C. necator* was performed following the protocol of Li et al. (57) with minor modifications. Precultures of 3 mL minimal medium with 2 % fructose were inoculated with freshly streaked cultures and shaken at 28 °C for 24 h. Main cultures of 10 mL minimal medium with 2 % fructose were inoculated to an OD<sub>600</sub> of 0.3 and shaken at 28 °C for 48 h. After 48 h, 200 µL of each culture was harvested by centrifugation at 4 000 rpm for 5 min. The pellets were washed in 400 µL of 0.9% NaCl and centrifuged again at 4 000 rpm for 5 min. The pellets were resuspended in 200 µL of 0.9% NaCl and 4 µL of Nile Red (1500 µg/mL in DMSO) were added. The mixtures were incubated in the dark for 30 min, then harvested and washed again in 200 µL NaCl.

For microscopy, agarose slides were prepared to ensure proper mounting of the cells. A 1% agarose solution in water was prepared, dissolved by boiling, and then poured over a glass slide. The agarose was allowed to solidify at room temperature. 2 µL of the washed cell pellet were pipetted onto the hardened agar and covered with a coverslip. Microscopic analysis of the strains was performed on a Zeiss Axio Imager.M2 using the EC Plan-Neofluar 100x/1.3 Oil M27 objective and LED module 567 as light source. For visualization of Nile red stained granule, excitation and emission wavelength were adjusted to 574-599 nm and 612-682 nm via optical filters. Whole cells were imaged in bright field mode.

#### **4.7 Plasmid loss**

To ensure the loss of the pCn-Red plasmid, a single colony of *C. necator* cells harboring pCn-Red was inoculated into 3 mL of minimal medium with gentamycin (culture 1) and incubated at 28 °C with shaking for 48 h. Then, 50 µL of culture 1 were used to inoculate a second 3 mL minimal medium culture with gentamycin (culture 2). Culture 2 again incubated at 28 °C with shaking for 48 h. The OD<sub>600</sub> of culture 2 was measured, and an appropriate dilution of the culture was plated on TSB agar with gentamycin to

obtain approximately 100 colonies. After incubation at 28 °C for 24 h, the resulting colonies were restreaked on TSB agar with and without tetracycline to identify clones that have lost the pCn-Red plasmid.



## 5. References

1. Pohlmann A, Fricke WF, Reinecke F, Kusian B, Liesegang H, Cramm R, et al. Genome sequence of the bioplastic-producing “Knallgas” bacterium *Ralstonia eutropha* H16. *Nat Biotechnol*. 2006 Oct;24(10):1257–62. doi: 10.1038/nbt1244
2. Panich J, Fong B, Singer SW. Metabolic engineering of *Cupriavidus necator* H16 for sustainable biofuels from CO<sub>2</sub>. Vol. 39, *Trends in Biotechnology*. Elsevier Ltd; 2021. p. 412–24. doi: 10.1016/j.tibtech.2021.01.001
3. Pan H, Wang J, Wu H, Li Z, Lian J. Synthetic biology toolkit for engineering *Cupriavidus necator* H16 as a platform for CO<sub>2</sub> valorization. Vol. 14, *Biotechnology for Biofuels*. BioMed Central Ltd; 2021. doi: 10.1186/s13068-021-02063-0
4. Gottschalk G, Eberhardt U, Schlegel HG. Verwertung von Fructose durch *Hydrogenomonas* H16 (I.). *Arch Mikrobiol*. 1964 Mar;48:95–108. doi: 10.1007/BF00406600
5. Lambauer V, Kratzer R. Lab-scale cultivation of *Cupriavidus necator* on explosive gas mixtures: carbon dioxide fixation into polyhydroxybutyrate. *Bioengineering*. 2022 May 1;9(5). doi: 10.3390/bioengineering9050204
6. Morlino MS, Serna García R, Savio F, Zampieri G, Morosinotto T, Treu L, et al. *Cupriavidus necator* as a platform for polyhydroxyalkanoate production: An overview of strains, metabolism, and modeling approaches. Vol. 69, *Biotechnology Advances*. Elsevier Inc.; 2023. doi : 10.1016/j.biotechadv.2023.108264
7. Grousseau E, Lu J, Gorret N, Guillouet SE, Sinskey AJ. Isopropanol production with engineered *Cupriavidus necator* as bioproduction platform. *Appl Microbiol Biotechnol*. 2014;98(9):4277–90. doi: 10.1007/s00253-014-5591-0
8. Collas F, Dronsella BB, Kubis A, Schann K, Binder S, Arto N, et al. Engineering the biological conversion of formate into crotonate in *Cupriavidus necator*. *Metab Eng*. 2023 Sep 1;79:49–65. doi: 10.1016/j.ymben.2023.06.015
9. Krieg T, Sydow A, Faust S, Huth I, Holtmann D. CO<sub>2</sub> to terpenes: autotrophic and electroautotrophic  $\alpha$ -humulene production with *Cupriavidus necator*. *Angewandte Chemie - International Edition*. 2018 Feb 12;57(7):1879–82. doi: 10.1002/anie.201711302
10. R. Simon, U. Priefer, A. Pühler. A broad host mobilization system for in vivo genetic engineering: transposon mutagenesis in gram negative bacteria. *Nat Biotechnol*. 1983 Nov;1:784–91. doi: 10.1038/nbt1183-784
11. Friedrich B, Hogrefe C, Schlegel HG. Naturally occurring genetic transfer of hydrogen-oxidizing ability between strains of *Alcaligenes eutrophus*. *J Bacteriol* [Internet]. 1981;147(1):198–205. doi: 10.1128/jb.147.1.198-205.1981

12. Lenz O, Lauterbach L, Frielingsdorf S. O<sub>2</sub>-tolerant [NiFe]-hydrogenases of *Ralstonia eutropha* H16: physiology, molecular biology, purification, and biochemical analysis. *Methods in Enzymology*. Academic Press Inc.; 2018. p. 117–51. doi: 10.1016/bs.mie.2018.10.008
13. Park HC, Lim KJ, Park JS, Lee YH, Huh TL. High frequency transformation of *Alcaligenes eutrophus* producing poly- $\beta$ -hydroxybutyric acid by electroporation. *Biotechnology Techniques*. Vol. 9. 1995. doi: 10.1007/BF00152996
14. Taghavi S, Van Der Lelie D, Mergeay M. Electroporation of *Alcaligenes eutrophus* with (mega) plasmids and genomic DNA fragments. *Appl Environ Microbiol* [Internet]. 1994;3585–91. doi: 10.1128/aem.60.10.3585-3591.1994
15. Xiong B, Li Z, Liu L, Zhao D, Zhang X, Bi C. Genome editing of *Ralstonia eutropha* using an electroporation-based CRISPR-Cas9 technique. *Biotechnol Biofuels*. 2018 Jun 20;11(1). doi: 10.1186/s13068-018-1170-4
16. Martinez-Morales F, Borges A, Martinez A, Shanmugam K, Ingram L. Chromosomal integration of heterologous DNA in *Escherichia coli* with precise removal of markers and replicons used during construction. *J. Bacteriol*. 1999;181:7143–7148. doi: 10.1128/jb.181.22.7143-7148
17. Vajente M, Clerici R, Ballerstedt H, Blank LM, Schmidt S. Using *Cupriavidus necator* H16 to provide a roadmap for increasing electroporation efficiency in non-model bacteria. 2024. doi: 10.1101/2024.05.27.596136
18. Li R, Li A, Zhang Y, Fu J. The emerging role of recombineering in microbiology. Vol. 3, *Engineering Microbiology*. Elsevier B.V.; 2023. doi: 10.1016/j.engmic.2023.100097
19. Corts A, Thomason LC, Costantino N, Court DL. Recombineering in non-model bacteria. *Curr Protoc*. 2022 Dec 1;2(12). doi: 10.1002/cpz1.605
20. Datta S, Costantino N, Zhou X, Court DL. Identification and analysis of recombineering functions from gram-negative and gram-positive bacteria and their phages. Vol. 5, *PNAS* February. 2008. doi: 10.1073/pnas.0709089105
21. Datta S, Costantino N, Court DL. A set of recombineering plasmids for gram-negative bacteria. *Gene*. 2006 Sep 1;379(1–2):109–15. doi: 10.1016/j.gene.2006.04.018
22. Datsenko KA, Wanner BL. One-step inactivation of chromosomal genes in *Escherichia coli* K-12 using PCR products. *Proc Natl Acad Sci* [Internet]. 2000;(12).doi 1073pnas.120163297
23. Madyagol M, Al-Alami H, Levarski Z, Drahovská H, Turňa J, Stuchlík S. Gene replacement techniques for *Escherichia coli* genome modification. Vol. 56, *Folia Microbiologica*. 2011. p. 253–63. doi: 10.1007/s12223-011-0035-z
24. Lee EC, Yu D, Martinez De Velasco J, Tessarollo L, Swing DA, Court DL, et al. A highly efficient *Escherichia coli*-based chromosome engineering system adapted for recombinogenic targeting and subcloning of BAC DNA. *Genomics*. 2001 Apr 1;73(1):56–65. doi: 10.1006/geno.2000.6451

25. Jia B, Yang JK, Liu WS, Li X, Yan YJ. Homologous overexpression of a lipase from *Burkholderia cepacia* using the lambda Red recombinase system. *Biotechnol Lett.* 2010;32(4):521–6. doi: 10.1007/s10529-009-0189-9
26. Lesic B, Rahme LG. Use of the lambda Red recombinase system to rapidly generate mutants in *Pseudomonas aeruginosa*. *BMC Mol Biol.* 2008 Feb 4;9. doi: 10.1186/1471-2199-9-20
27. Kang Y, Norris MH, Wilcox BA, Tuanyok A, Keim PS, Hoang TT. Knockout and pullout recombineering for naturally transformable *Burkholderia thailandensis* and *Burkholderia pseudomallei*. *Nat Protoc.* 2011 Aug;6(8):1085–104. doi: 10.1038/nprot.2011.346
28. Arhar S, Rauter T, Stolterfoht-Stock H, Lambauer V, Kratzer R, Winkler M, et al. CO<sub>2</sub>-based production of phytase from highly stable expression plasmids in *Cupriavidus necator* H16. *Microb Cell Fact.* 2024 Dec 1;23(1). doi: 10.1186/s12934-023-02280-2
29. Alagesan S, Hanks EKR, Malys N, Ehsaan M, Winzer K, Minton NP. Functional genetic elements for controlling gene expression in *Cupriavidus necator* H16. *Appl Environ Microbiol.* 2018 Oct 1;84(19). doi: 10.1128/AEM.00878-18
30. Sydow A, Pannek A, Krieg T, Huth I, Guillouet SE, Holtmann D. Expanding the genetic tool box for *Cupriavidus necator* by a stabilized L-rhamnose inducible plasmid system. *J Biotechnol.* 2017 Dec 10;263:1–10. doi: 10.1016/j.jbiotec.2017.10.002
31. Thomason LC, Costantino N, Li X, Court DL. Recombineering: genetic engineering in *Escherichia coli* using homologous recombination. *Curr Protoc.* 2023 Feb 1;3(2). doi: 10.1002/cpz1.656
32. Poteete AR, Fenton AC, Nadkarni A. Chromosomal duplications and cointegrates generated by the bacteriophage lambda Red system in *Escherichia coli* K-12. *BMC Mol Biol.* 2005 Dec 13;5. doi: 10.1186/1471-2199-5-22
33. Lenz O, Friedrich B. A novel multicomponent regulatory system mediates H<sub>2</sub> sensing in *Alcaligenes eutrophus*. *Proc Natl Acad Sci USA.* 1998;95:12474–9. doi: 10.1073/pnas.95.21.12474
34. Budde CF, Riedel SL, Willis LB, Rha CK, Sinskey AJ. Production of poly(3-hydroxybutyrate-co-3-hydroxyhexanoate) from plant oil by engineered *Ralstonia eutropha* strains. *Appl Environ Microbiol.* 2011 May;77(9):2847–54. doi: 10.1128/AEM.02429-10
35. Voss I, Steinbüchel A. Application of a KDPG-aldolase gene-dependent addition system for enhanced production of cyanophycin in *Ralstonia eutropha* strain H16. *Metab Eng.* 2006 Jan;8(1):66–78. doi: 10.1016/j.ymben.2005.09.003
36. Wang HH, Church GM. Multiplexed genome engineering and genotyping methods: Applications for synthetic biology and metabolic engineering. *Methods in Enzymology.* Academic Press Inc.; 2011. p. 409–26. doi: 10.1016/B978-0-12-385120-8.00018-8

37. Schlegel HG, Lafferty R, Krauss I. The isolation of mutants not accumulating poly-beta-hydroxybutyric acid. *Arch Mikrobiol.* 1970;71:283–94. doi: 10.1007/BF00410161
38. Murphy KC. Use of bacteriophage recombination functions to promote gene replacement in *Escherichia coli*. *J Bacteriol.* 1998;180(8):2063–71. doi: 10.1128/JB.180.8.2063-2071
39. Blank K, Hensel M, Gerlach RG. Rapid and highly efficient method for scarless mutagenesis within the *Salmonella enterica* chromosome. *PLoS One.* 2011;6(1). doi: 10.1371/journal.pone.0015763
40. Gerlach RG, Jäckel D, Hölzer SU, Hensel M. Rapid oligonucleotide-based recombineering of the chromosome of *Salmonella enterica*. *Appl Environ Microbiol.* 2009 Mar;75(6):1575–80. doi: 10.1128/AEM.02509-08
41. Chen C, Wei D, Liu P, Wang M, Shi J, Jiang B, et al. Inhibition of recBCD in *Klebsiella pneumoniae* by gam and its effect on the efficiency of gene replacement. *J Basic Microbiol.* 2016 Feb 1;56(2):120–6. doi: 10.1002/jobm.201400953
42. Huang TW, Lam I, Chang HY, Tsai SF, Palsson BO, Charusanti P. Capsule deletion via a  $\lambda$ -Red knockout system perturbs biofilm formation and fimbriae expression in *Klebsiella pneumoniae* MGH 78578. *BMC Res Notes* 2014. doi: 10.1186/1756-0500-7-13
43. Yin J, Zheng W, Gao Y, Jiang C, Shi H, Diao X, et al. Single-stranded DNA-binding protein and exogenous recBCD inhibitors enhance phage-derived homologous recombination in *Pseudomonas*. *iScience.* 2019 Apr 26;14:1–14. doi: 10.1016/j.isci.2019.03.007
44. Wang X, Zhou H, Chen H, Jing X, Zheng W, Li R, et al. Discovery of recombinases enables genome mining of cryptic biosynthetic gene clusters in *Burkholderiales* species. *Proc Natl Acad Sci U S A.* 2018 May 1;115(18):E4255–63. doi: 10.1073/pnas.1720941115
45. Lim HN, Lee Y, Hussein R. Fundamental relationship between operon organization and gene expression. *Proc Natl Acad Sci U S A.* 2011 Jun 28;108(26):10626–31. doi: 10.1073/pnas.1105692108
46. Dillingham MS, Kowalczykowski SC. RecBCD enzyme and the repair of double-stranded DNA breaks. *Microbiology and Molecular Biology Reviews.* 2008 Dec;72(4):642–71. doi: 10.1128/mmbr.00020-08
47. Guzman LM, Belin D, Carson MJ, Beckwith J. Tight regulation, modulation, and high-level expression by vectors containing the arabinose PBAD promoter. *J Bacteriol.* 1995;177(14):4121–30. doi: 10.1128/jb.177.14.4121-4130.1995
48. Ares-Arroyo M, Rocha EPC, Gonzalez-Zorn B. Evolution of ColE1-like plasmids across  $\gamma$ -Proteobacteria: from bacteriocin production to antimicrobial resistance. *PLoS Genet.* 2021 Nov 30;17(11). doi: 10.1371/journal.pgen.1009919

49. Schwartz E, Darnedde J, Eiting M, Friedrich B. The *Alcaligenes eutrophus* H16 *hoxX* gene participates in hydrogenase regulation. Vol. 176, J Bacteriol. 1994. doi: 10.1128/jb.176.14.4385-4393.1994
50. Gruber S, Schwendenwein D, Magomedova Z, Thaler E, Hagen J, Schwab H, et al. Design of inducible expression vectors for improved protein production in *Ralstonia eutropha* H16 derived host strains. Vol. 235, Journal of Biotechnology. Elsevier B.V.; 2016. p. 92–9. doi: 10.1016/j.jbiotec.2016.04.026
51. Ehsaan M, Baker J, Kovács K, Malys N, Minton NP. The pMTL70000 modular, plasmid vector series for strain engineering in *Cupriavidus necator* H16. J Microbiol Methods. 2021 Oct 1;189. doi: 10.1016/j.mimet.2021.106323
52. Miksch G, Kleist S, Friehs K, Flaschel E. Overexpression of the phytase from *Escherichia coli* and its extracellular production in bioreactors. Appl Microbiol Biotechnol. 2002;59(6):685–94. doi: 10.1007/s00253-002-1071-z
53. Romano N, Kumar V. Phytase in animal feed. Enzymes in human and animal nutrition: Principles and Perspectives. Elsevier Inc.; 2018. p. 73–88. doi: 10.1016/B978-0-12-805419-2.00004-6
54. Keating KW, Young EM. Systematic part transfer by extending a modular toolkit to diverse bacteria. ACS Synth Biol. 2023 Jul 21;12(7):2061–72. doi: 10.1021/acssynbio.3c00104
55. Gibson DG, Young L, Chuang RY, Venter JC, Hutchison CA, Smith HO. Enzymatic assembly of DNA molecules up to several hundred kilobases. Nat Methods. 2009;6(5):343–5. doi: 10.1038/nmeth.1318
56. Saheki S, Takeda A, Shimazu T. Assay of inorganic phosphate in the mild pH range, suitable for measurement of glycogen phosphorylase activity. Anal Biochem. 1985;148:277–305. doi: 10.1016/0003-2697(85)90229-5
57. Li M, Wilkins M. Flow cytometry for quantitation of polyhydroxybutyrate production by *Cupriavidus necator* using alkaline pretreated liquor from corn stover. Bioresour Technol. 2020 Jan 1;295. doi: 10.1016/j.biortech.2019.122254
58. Jiang Y, Chen B, Duan C, Sun B, Yang J, Yang S. Multigene editing in the *Escherichia coli* genome via the CRISPR-Cas9 system. Appl Environ Microbiol. 2015;81(7):2506–14. doi: 10.1128/AEM.04023-14
59. Bolivar F, Rodriguf RL, Greene PJ, Betlaci-I MC, Heyneker HB, Boyer HW, et al. Construction and characterization of new cloning vehicles II. A multipurpose cloning system. Gene. 1977;2:95–113.

## 6. Supporting information

The supporting information contains a detailed description of the three targeted *C. necator* loci (Table S1), a list of all plasmids used and prepared during this study (Table S2), and detailed descriptions of cloning strategies (Table S3 – S11). Further, additional data concerning the *appA* integration studies, along with the corresponding figures (Figure S1 – S5), is provided.

### 6.1 Loci targeted in this work

Table S1: *C. necator* loci information, including their RefSeq, location, locus tag and chromosome number.

| Gene         | RefSeq-Protein | Location          | Locus tag | Chromosome Nr. |
|--------------|----------------|-------------------|-----------|----------------|
| <i>proC</i>  | WP_011615991.1 | 3359051...3359887 | H16_A3106 | 1              |
| <i>eda</i>   | WP_010814144.1 | 1370637...1371281 | H16_B1213 | 2              |
| <i>phaC1</i> | WP_013956451.1 | 1556003...1557772 | H16_A1437 | 1              |

### 6.2 Plasmids used in this work

Table S2: Plasmids used in this work, including a description of their most important features, their application and source.

| Plasmid             | Description  | Application   | Source                            |
|---------------------|--|---|-----------------------------------|
| pCas                | Km <sup>R</sup> , P <sub>BAD</sub> , lambda RED genes ( <i>gam</i> , <i>beta</i> , <i>exo</i> ), pSC101 ori, Rep101, SpyCas9, gRNA | Template for amplification: <i>beta</i> , <i>exo</i> , <i>gam</i>                                 | Addgene #62225<br>Jiang 2015 (58) |
| pKRSF1010           | Km <sup>R</sup> , RSF101 ori, RSF101 mob and ori   | Template for amplification: kanR  | Gruber 2016 (50)                  |
| pINT_lacY_Phac_loxP | Cm <sup>R</sup> , pK470MobRP4, P <sub>H16 B1772</sub> , lacY, <i>phaC1</i> homologous regions, loxP sites                          | vector backbone used for <i>eGFP</i> integration  | Gruber 2016 (50)                  |
| pBR322              | Tet <sup>R</sup> , Amp <sup>R</sup> , pMB1 ori, <i>rop</i>   | Template for amplification: tetR  | NEB #N3033S<br>Bolivar 1977 (59)  |
| pKESa               | Km <sup>R</sup> P <sub>T5</sub> , eGFP, pSa ori  | Template for amplification: pSa   | Arhar 2024 (28)                   |
| pKPrepPar_Pj5       | Km <sup>R</sup> , P <sub>J5</sub> , <i>E. coli</i> AppA, pBBR1 ori, par  | Template for amplification: appA  | Arhar 2024 (28)                   |
| pLO3                | Tet <sup>R</sup> , SacB, RP4 transfer ori, pBR322 ori  | Template for amplification: ori pLO3  | Lenz 1998 (33)                    |
| pCM_Cre             | Cm <sup>R</sup> , P <sub>Tac</sub> , mob, colE1, cre, cym <sup>R</sup>   | Template for amplification: CmR + P <sub>Tac</sub> + cre + cym <sup>R</sup>                       | Gruber 2016 (50)                  |
| pINT_eGFP_Phac_loxP | Cm <sup>R</sup> , pK470MobRP4, P <sub>T5</sub> , eGFP, <i>phaC1</i> homologous regions, loxP sites                                 | Integration of an <i>eGFP</i> expression cassette into <i>phaC1</i>                               | This study                        |
| pCn-Red             | Tet <sup>R</sup> , pSa ori, P <sub>Rha</sub> , <i>beta</i> , <i>exo</i> , <i>gam</i> , <i>rhaS</i> , <i>rhaR</i>                   | Induced expression of the lambda RED system in <i>C. necator</i>                                  | This study                        |
| pHRep-HKH1          | Km <sup>R</sup> , pLO3 ori, <i>phaC1</i> homologous regions  | Replacement of <i>eGFP</i> /disruption of <i>phaC1</i> , vector backbone for pHInt-AppA-KanR-loxP | This study                        |

|                      |  |   |            |
|----------------------|--|---|------------|
| pHRep-HKH-ProC       | Km <sup>R</sup> , pLO3 ori, <i>proC</i> homologous regions   | Replacement of <i>proC</i>                                | This study |
| pHRep-HKH-Eda        | Km <sup>R</sup> , pLO3 ori, <i>eda</i> homologous regions  | Replacement of <i>eda</i>                                 | This study |
| pHInt-AppA-KanR-loxP | Km <sup>R</sup> , pLO3 ori, loxP sites, <i>phaC1</i> homologous regions, P <sub>J5</sub> <i>appA</i> | Disruption of <i>phaC1</i> via integration of <i>appA</i> | This study |
| pCn-Cre              | Cm <sup>R</sup> , pLO3 ori, Cre recombinase, Cym <sup>R</sup> , P <sub>Tac-CymO</sub>                | Production of cre recombinase for marker recycling        | This study |

### 6.3 Cloning of plasmids used in this study

The fragments *PhaC1* 5', *PhaC1* 3', *ProC* 5', *ProC* 3', *Eda* 5' and *Eda* 3' were amplified from the genomic DNA (gDNA) of *C. necator* H16 wild-type.

#### Plasmid pINT\_eGFP\_PhaC\_loxP

For construction of a conjugational suicide plasmid to integrate an *eGFP* cassette into the *phaC1* locus, the previously published pINT\_lacY\_phaC-loxP (Table S2) plasmid was digested with *SphI* and *HindIII* to excise the *lacY* expression cassette. The *eGFP* cassette, containing the T5 promotor and the target gene, was amplified from pKESa by using primers pCR-Int-eGFP\_f1/r1 and used for Gibson assembly with the digest backbone. The final construct was verified via restriction digest and Sanger sequencing using primers pSEQ-plnt-phaC\_f1 and pSEQ-plnt-CmR\_r1. Correct genomic integration was investigated by colony PCR using primers pCont\_phaC1\_f2/r2, and sequencing of the corresponding DNA fragment.

| Application                | Primer name       | Sequence   |
|----------------------------|-------------------|--|
| PCR: P <sub>T5</sub> -eGFP | pCR-Int-eGFP_f1   | gcagcacctgggacgactactagtgcATCATAAAAAATTATTGCTTTGTGAGCG |
|                            | pCR-Int-eGFP_r1   | cttctctcatccgcaaacagccaagctt TACTTGTACAGCTCGTCCATGC    |
| Colony PCR                 | pCont_phaC1_f2    | GGA GCC GGT TCG AAT AGT GAC                            |
|                            | pCont_phaC1_r2    | GAC AAC GTC AGT CAT TGT GTA GTC                        |
| Sequencing                 | pSEQ-plnt-phaC_f1 | gtactacatcctggacctgcag                                 |
|                            | pSEQ-plnt-CmR_r1  | CTTCCGTACAGGTATTTATTCGTC                               |

#### Plasmid pCn-Red

The plasmid pCn-Red was constructed by Gibson Assembly of the following PCR products. The pSa ori was amplified from the plasmid pKESa (Table S2) using primer pCR-pCn-RED-SaOri\_f1/r1 (Table S3). The tetracycline resistance cassette was amplified from plasmid pBR322 (Table S2) using primer pCR-pCn-RED-TetR\_f1/r1 (Table S3). Promoter P<sub>Rha</sub> with regulators *rhaR/S* was amplified from genomic DNA of *E. coli* MG1655 (Table S2) using primer pCR-Reco-rha\_f1/r1 (Table S3). *Beta*, *exo* and *gam* were amplified from plasmid pCas (Table S2) using primer pCR-Beta\_f1/r1, pCR-Exo\_f1/r1 and pCR-Gam\_f1/r1 (Table S3), respectively. Correct assembly was confirmed by Sanger sequencing using the primer pSeq-pSa-Rep\_f1b, pSeq-rhaR\_r1, pSeq-rhaS\_r1, pSeq-PrhaB\_r1 and pSeq-TetR\_r1 (Table S3).

Table S3: Primer used to construct pCn-Red.

| Application                         | Primer name          | Sequence   |
|-------------------------------------|----------------------|--|
| PCR: TetR                           | pCR-pCn-RED-TetR_f1  | CCGAAAAGTGCCACCTGACG   |
|                                     | pCR-pCn-RED-TetR_r1  | agtttgAGATCTTTAATTAAtttatgtgatATTTAAATTGGAGTGGTGAATCCGTTAGC                                    |
| PCR: pSa                            | pCR-pCn-RED-SaOri_f1 | TAAATatcacataaaTTAATTAAAGATCTcaaactgtacGTTTAAACgctactttcgaacgactcctg                           |
|                                     | pCR-pCn-RED-SaOri_r1 | Cctgcagggcagaccagaaccaatcctattc  |
| PCR: P <sub>RHA</sub> + rhaR + rhaS | pCR-Reco-rha_f1      | ccttcgttaggtgctgaataggattggttctggtctgccctgcaggTCTAGAcgcagaaaggcccacc                           |
|                                     | pCR-Reco-rha_r1      | ATGTATATCTCCTTCTTAAGAATTGTTTCATTACGACCAGTCTAAAAAGCg  |
| PCR: Beta                           | pCR-Beta_f1          | ACTGGTCGTAATGAACAATTCTTAAGAAGGAGATATACAT atgagtactgcactcgcaac                                  |
|                                     | pCR-Beta_r1          | catcgatcccgtgacgctgcaggataatgccggtgcatGGTTGTCCTCCTTT tcatgctgccacctctg                         |
| PCR: Exo                            | pCR-Exo_f1           | atgacaccggacattatcctg  |
|                                     | pCR-Exo_r1           | aatgcttttgcttgatctcagttcagttatataatccatGGTTGTCCTCCTTT tcatgccattgctccc                         |
| PCR: Gam                            | pCR-Gam_f1           | atggatattaatactgaaactgagatcaagc  |
|                                     | pCR-Gam_r1           | AATGGTTTCTTAGACGTCAGGTGGCACTTTTCGGAAAAGGCCATCCGTCAGGATGG<br>CCTTCTttatacctctgaatcaatatcaacctgg |
| Sequencing                          | pSeq-pSa-Rep_f1b     | gaattaaataccctgttgcggtatag   |
|                                     | pSeq-rhaR_r1         | CAGTCAAGATTTCAGCTTCAGACG   |
|                                     | pSeq-rhaS_r1         | CTGCTGTTCCATCTGTGCAACC   |
|                                     | pSeq-PrhaB_r1        | CAAATTGTGAACATCATCACGTTTCATC   |
|                                     | pSeq-TetR_r1         | CTTATCGATGATAAGCTGTCAAACATG  |

### Suicide plasmid pHRep-HKH1

The suicide plasmid pHRep-HKH1 was constructed using Gibson Assembly. The origin of replication was amplified from the plasmid pLO3 (Table S2) with the primers pCR-HKH1-ColE1\_f1/r1 (Table S4). The kanamycin resistance cassette was amplified from the plasmid pKRSF1010 (Table S2) using primer pCR-HKH1-KanR\_f1/r1 (Table S4). *PhaC1* 5' and *PhaC1* 3' homologous regions were amplified from the gDNA of *C. necator* H16 wildtype (H16\_A1437, see Table S1) using primer pCR-HKH1-phaC1-1\_f1/r1 and pCR-HKH1-phaC1-2\_f1/r1 (Table S4), respectively. Correct assembly was confirmed by Sanger sequencing using primer pSeq-KanR\_f1, pSeq-plnt-phaC\_f1, pCont\_phaC1\_r1, pSeq-KanR\_r1, pCont\_BB\_f1 and pSeq-phaC1\_2\_f1 (Table S4). After transformation into *C. necator* (procedure outlined in Materials and Methods section 4.2), the replacement of the genomic *eGFP* was determined via colony PCR using the primer pCont\_phaC1\_f2/r2 (Table S4).

Table S4: Primer used to construct pHRep-HKH1.

| Application   | Primer name         | Sequence   |
|---------------|---------------------|--|
| PCR: ori pLO3 | pCR-HKH1-ColE1_f1   | aagccaaggcatgaCTCGAG ATGTGAGCAAAAGGCCAGCAAAAG      |
|               | pCR-HKH1-ColE1_r1   | ggtcgccatTCTAGA CCCGTAGAAAAGATCAAAGGATCTTCTTGAG    |
| PCR: KanR     | pCR-HKH1-KanR_f1    | tgggacgactGAATTC ttgctgttctacaactctttgtttatcttc    |
|               | pCR-HKH1-KanR_r1    | gccgcgtgctcgtatGGATCC aaggccatccgtcctaggag         |
| PCR: phaC1_1  | pCR-HKH1-phaC1-1_f1 | AAGATCCTTTGATCTTTTCTACGGGTCTAGA atggcgaccggcaaggcg |
|               | pCR-HKH1-phaC1-1_r1 | caaaagagttgtagaaacgcaaaGAATTC agtcgtcccagggtgctgc  |
| PCR: phaC1_2  | pCR-HKH1-phaC1-2_f1 | cctaggacggatggccttGGATCC acatcgagcacgcggccatc      |



|            |                     |  |
|------------|---------------------|--|
|            | pCR-HKH1-phaC1-2_r1 | TGCTGGCCTTTTGCTCACATCTCGAG tcatgccttggtttgacgtatcg |
| Colony PCR | pCont_phaC1_f2      | GGA GCC GGT TCG AAT AGT GAC                        |
|            | pCont_phaC1_r2      | GAC AAC GTC AGT CAT TGT GTA GTC                    |
| Sequencing | pSeq-KanR_f1        | GCCTCGGTGAGTTTTCTCCTTC                             |
|            | pSEQ-plnt-phaC_f1   | gtactacatcctggacctgcag                             |
|            | pCont_phaC1_r1      | CGCGGTGAGACAATGGTG                                 |
|            | pSeq-KanR_r1        | CTAGAGCAAGACGTTTCCCGTTG                            |
|            | pCont_BB_f1         | CCA CCT CTG ACT TGA GCG TCG                        |
|            | pSeq-phaC1_2_f1     | atcgagcatcacggcagctg                               |

### Linear fragment PCR-HKH1

The linear fragment PCR-HKH1 was amplified using the suicide plasmid pHRep-HKH1 as a template with the primers plnt-phaC1-eGFPlin\_f1/r1 (Table S5). After transformation into *C. necator* (procedure outlined in Materials and Methods section 4.2), the replacement of genomic *eGFP* was determined via colony PCR using the primer pCont\_phaC1\_f2/r2 (Table S4).

Table S5: Primer used to construct PCR-HKH1.

| Application                           | Primer name           | Sequence                 |
|---------------------------------------|-----------------------|--------------------------|
| PCR: amplification of linear fragment | plnt-phaC1-eGFPlin_f1 | ATGGCGACCGGCAAAGGCG      |
|                                       | plnt-phaC1-eGFPlin_r1 | TCATGCCTTGGCTTTGACGTATCG |

### Suicide plasmid pHRep-HKH-ProC

For the construction of suicide plasmid pHRep-HKH-ProC, pLO3 origin of replication and the kanamycin resistance cassette of plasmid pHRep-HKH1 were amplified using primers pCR-ori\_pLO3\_f2/r2 and pCR-Hrep-Kan\_f2/r2. *ProC* 5' and *proC* 3' were amplified from the gDNA of *C. necator* H16 wildtype (H16\_A3106, see Table S1) using primer pCR-HRep-proC-5'\_f1/r1 and pCR-HRep-proC-3'\_f1/r1 (Table S6), respectively. Correct assembly was confirmed by Sanger sequencing using six different primers. After transformation into *C. necator* (procedure outlined in Materials and Methods section 4.2), the replacement of the genomic *proC* was determined via colony PCR using the primer pCont\_proC\_f1 and pSeq-KanR\_r1 (Table S6).

Table S6: Primer used to construct pHRep-HKH-ProC.

| Application   | Primer name         | Sequence  |
|---------------|---------------------|---|
| PCR: ori pLO3 | pCR-ori_pLO3_f2     | CTCGAGATGTGAGCAAAAGGCCAGCAAAAG                                |
|               | pCR-ori_pLO3_r2     | TCTAGACCCGTAGAAAAGATCAAAGGATCTTCTTGAG                         |
| PCR: KanR     | pCR-Hrep-Kan_f2     | GAATTCttgcgtttctacaaactctttgttatttttc                         |
|               | pCR-Hrep-Kan_r2     | AGATCT aaggccatccgtcctaggag                                   |
| PCR: ProC 5'  | pCR-HRep-proC-5'_f1 | TCTCAAGAAGATCCTTTGATCTTTTCTACGGGTCTAGAACATCCTTGTCGTCATCGAGG   |
|               | pCR-HRep-proC-5'_r1 | aaaataaacaaaagagttgtagaacgcaaaGAATTC ATCGAGCATGGAGATCCGTTGG   |
| PCR: ProC 3'  | pCR-HRep-proC-3'_f1 | tgagcgtcagacaggcctcctaggacggatggccttAGATCT ATTGAGGCGCGGCCAAAC |
|               | pCR-HRep-proC-3'_r1 | TACGGTTCTGGCCTTTTGCTGGCCTTTTGCTCACATCTCGAGGCACGCTGCTGCTGCTG   |
| Colony PCR    | pCont-proC_f1       | TGTCGCTCATGATGTCGTACAC  |
|               | pSeq-KanR_r1        | CTAGAGCAAGACGTTTCCCGTTG                                       |
| Sequencing    | pSeq-KanR_r1        | CTAGAGCAAGACGTTTCCCGTTG                                       |
|               | pSeq-ori-pLO3_f1    | AAAGAGTTGGTAGCTCTTGATCCG                                      |
|               | pSeq-KanR_f1        | GCCTCGGTGAGTTTTCTCCTTC  |
|               | pCont_BB_f1         | CCA CCT CTG ACT TGA GCG TCG                                   |
|               | pCR-Hrep-Kan_f2     | GAATTCttgcgtttctacaaactctttgttatttttc                         |
|               | pCR-ori_pLO3_f2     | CTCGAGATGTGAGCAAAAGGCCAGCAAAAG                                |

### Linear fragment PCR-HKH-ProC

The amplification of the kanamycin resistance cassette and of the elements *proC* 5' and *proC* 3' is outlined in Table S6. These are the same elements used for the construction of the suicide plasmid pHRep-HKH-ProC. The fragment for transformation into *C. necator* was generated via overlap extension PCR using the primers pRec-ProC\_f2/r2 (Table S7). After transformation (procedure outlined in Materials and Methods section 4.2), the replacement of genomic *proC* was determined via colony PCR using the primer pCont\_proC\_f1 and pSeq-KanR\_r1 (Table S6).

Table S7: Primer used to construct PCR-HKH-ProC.

| Application           | Primer name   | Sequence              |
|-----------------------|---------------|-----------------------|
| Overlap extension PCR | pRec-ProC1_f2 | ACATCCTTGTCGTCATCGAGG |
|                       | pRec-ProC1_r2 | GCACGCTGCTGCTGCTG     |

### Suicide plasmid pHRep-HKH-Eda

For the construction of suicide plasmid pHRep-HKH-Eda, the pLO3 origin of replication and *kanR* for the construction of plasmid pHRep-HKH1 were reused (primer for *ori* and *kanR* see Table S6). *Eda* 5' and *eda* 3' were amplified from the gDNA of *C. necator* H16 wildtype (H16\_B1213, see Table S1) using primer pCR-HRep-eda-5'\_fw/rv and pCR-HRep-eda-3'\_fw/rv, respectively (Table S8). Correct assembly was confirmed by Sanger sequencing using the same six primers as for the *proC* plasmid (Table S6). After transformation into *C. necator* (procedure outlined in Materials and Methods section 4.2), the replacement of the genomic *eda* was determined via colony PCR using the primer pCont-eda\_f1 and pCR-Rep-eda-3in1\_r1 (Table S8).

Table S8: Primer used to construct pHRep-HKH-Eda.

| Application | Primer name         | Sequence  |
|-------------|---------------------|---|
| PCR: Eda 5' | pCR-HRep-eda-5'_f1  | GGATCTCAAGAAGATCCTTTGATCTTTTCTACGGGTCTAGACATCGCGCTACCTGCAAGG  |
|             | pCR-HRep-eda-5'_r1  | aaaaataaacaaaagagttgtagaaacgcaaaGAATTC TCAGGGAAGCAGGAGTTCAGG  |
| PCR: Eda 3' | pCR-HRep-eda-3'_f1  | gagcgtcagacaggcctcctagtagcggtggccttAGATCT GAGAAACGGCACGCCATGC |
|             | pCR-HRep-eda-3'_r1  | CGGTTCTGGCCTTTTGCTGGCCTTTTGCTCACATCTCGAGCCGCTGCAATTCACCCTGC   |
| Colony PCR  | pCont-eda_f1        | GAACCGCTGGTGGAGTTCAAC   |
|             | pCR-Rep-eda-3in1_r1 | CATGGCGTGCCGTTTCTC  |

### Linear fragment PCR-HKH-Eda

Amplification of the kanamycin resistance cassette is outlined in Table S6, amplification of the fragments *eda* 5' and *eda* 3' is outlined in Table S8. These are the same fragments present on the respective suicide plasmid pHRep-HKH-Eda. The linear fragment was assembled by overlap extension PCR using the primer pRec-eda-fw1/rv1 (Table S9). After transformation into *C. necator* (procedure outlined in Materials and Methods section 4.2), the replacement of the genomic *eda* was determined via colony PCR using the primer pCont-eda\_f1 and pCR-Rep-eda-3in1\_r1 (Table S8).

Table S9: Primer used to construct PCR-HKH-Eda.

| Application           | Primer name | Sequence            |
|-----------------------|-------------|---------------------|
| Overlap extension PCR | pRec-eda-f1 | CATCGCGCTACCTGCAAGG |
|                       | pRec-eda-r1 | CCGCTGCAATTCACCCTGC |

### Suicide plasmid pHInt-AppA-KanR-loxP

The suicide plasmid pHInt-AppA-kanR-loxP was constructed using Gibson Assembly. The plasmid pHRep-HKH1 was used as backbone with *kanR* being excised using restriction enzymes *EcoRI* and *BamHI*. The fragment *appA* including one loxP site was amplified from the plasmid pKPrepPar\_Pj5 (Table S2) using primer pCR-AppA-loxP-PhaC\_f1 and pCR-AppA-loxP\_r1 (Table S10) with the loxP site being added as primer overhang. *KanR* including the second loxP site was amplified from the plasmid pHRep-HKH1 with loxP using primer pCR-KanR-loxP-PhaC\_f1 and primer pCR-KanR-loxP\_r1 (Table S10) with again the loxP site being added as primer overhang. Correct assembly was confirmed by Sanger sequencing using primer pSeq-ori-pLO3\_f1, pSeq-KanR\_r1, pSeq-rrnBT\_r1 and pSeq-rrnBT\_f1 (Table S10). After transformation into *C. necator* (procedure outlined in Materials and Methods section 4.2), the replacement of the genomic *phaC1* and *eGFP*, respectively, was determined via colony PCR using the primer pCont-PhaC1\_f4/r4 (Table S10).

Table S10: Primer used to construct plasmid pHInt-AppA-KanR-loxP.

| Application      | Primer name           | Sequence  |
|------------------|-----------------------|---|
| PCR: AppA + loxP | pCR-AppA-loxP-PhaC_f1 | gacgccagcatggccggcagcacctgggacgactGCATGCaaaaaccgttattgacacag                                |
|                  | pCR-AppA-loxP_r1      | aaacaaaagagattgttagaaacgcaaaCATATGataacttcgtatagcatattacgaagttatTTAATT<br>AAaaggccatccgtcag |
| PCR: KanR + loxP | pCR-KanR-loxP-PhaC_f1 | CATATGtttcggttctacaaactctttgttt   |
|                  | pCR-KanR-loxP_r1      | cttcgatggcgcgatggccgctgctcgatgtataacttcgtatagcatattacgaagttatACTAGT<br>aaggccatccgtcctag    |
| Colony PCR       | pCont-PhaC1_f4        | CTTCCAGCCAGTTCCAGG  |
|                  | pCont-PhaC1_r4        | GACTTCGCTCACCTGCTC  |
|                  | pSeq-phaC1_f1         | atcgagcatcacggcagctg  |
|                  | pSeq-phaC1_r1         | ctggaagtactcgttctgaagac   |
| Sequencing       | pSeq-ori-pLO3_f1      | AAAGAGTTGGTAGCTCTTGATCCG  |
|                  | pSeq-KanR_r1          | CTAGAGCAAGACGTTTCCCGTTG   |
|                  | pSeq-rrnBT_r1         | cgttcactctgagttcgcatg   |
|                  | pSeq-rrnBT_f1         | gcggattgaacgttgcaagc  |

### Linear fragment pHInt-AppA-KanR-loxP

The linear fragment pHInt-AppA-KanR-loxP was amplified from the respective suicide plasmid pHInt-AppA-KanR-loxP using primer pInt-phaC1-eGFPlin\_f1/r1 (Table S5). After transformation into *C. necator* (procedure outlined in Materials and Methods section 4.2), the replacement of genomic *phaC1* and *eGFP*, respectively was determined via colony PCR using the primer pCont-phaC1\_f4/r4 (Table S10).

## Plasmid pCn-Cre

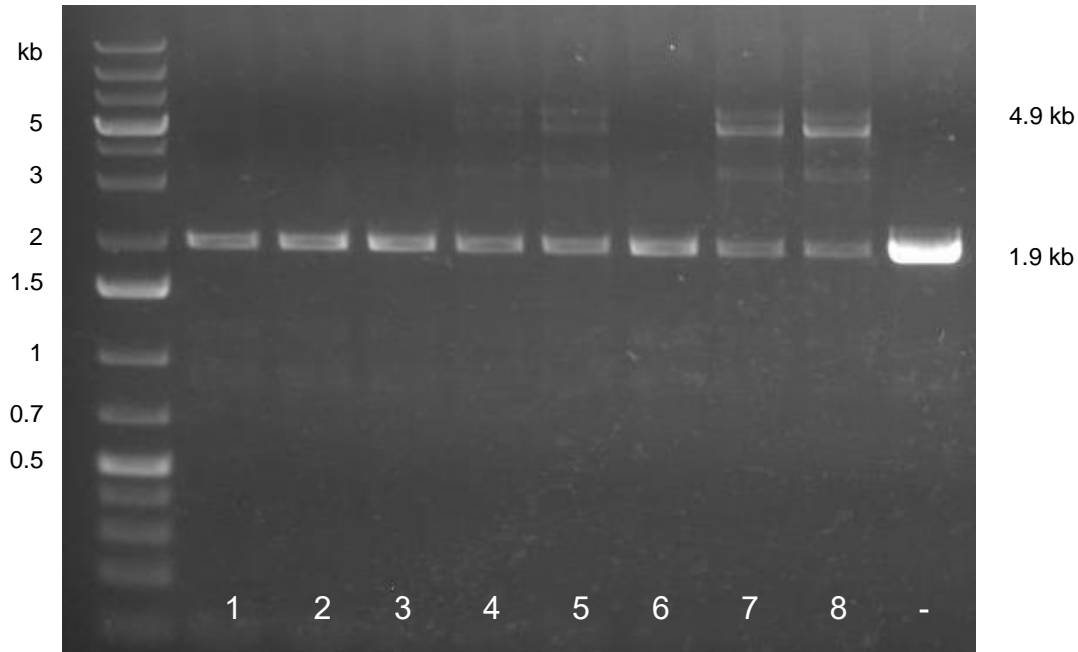
The plasmid pCn-Cre was constructed using Gibson Assembly. The fragment comprising  $P_{TAC}$ , the Cre recombinase, cmR and cymR was amplified from the plasmid pCM\_Cre (Table S2) using primers pCR-CymR-pLO3\_f1 and pCR-pCnIC-CmR\_r1 (Table S11), respectively. The pLO3 origin of replication was amplified from plasmid pLO3 (Table S2) using the primers pCR-pCnIC-ori\_f1 and pCR-pCnIK-ori\_r1 (Table S11). Correct assembly was confirmed by Sanger sequencing using primer pSeq-ori-pLO3\_f1 and pSEQ-plnt-CmR\_r1 (Table S11).

Table S11: primer used to construct plasmid pCn-Cre.

| Application   | Primer name      | Sequence  |
|---|------------------|---|
| PCR: $P_{tac}$ + cre + cm <sup>R</sup> + cym <sup>R</sup> | pCR-CymR-pLO3_f1 | AAGGATCTCAAGAAGATCCTTTGATCTTTTCTACGGGGTCGAC<br>acggatggccttttgc |
|   | pCR-pCnIC-CmR_r1 | CCTGGCCTTTTGCTGGCCTTTTGCTCACATttaactggcctcaggcatttg             |
| PCR: ori pLO3   | pCR-pCnIC-ori_f1 | ATGTGAGCAAAAGGCCAGC   |
|   | pCR-pCnIK-ori_r1 | CCCGTAGAAAAGATCAAAGGATCTTC                                      |
| Sequencing  | pSeq-ori-pLO3_f1 | AAAGAGTTGGTAGCTCTTGATCCG  |
|   | pSEQ-plnt-CmR_r1 | CTCCGTCACAGGTATTTATTCGTC  |

## 6.4 Additional data

The suicide plasmid pHInt-AppA-KanR-loxP was transformed into *C. necator* H16 wildtype, with the transformants being selected on kanamycin containing agar plates as we intended to integrate the cassette containing *appA* and *kanR* into the *phaC1* locus. Transformants were screened for correct integration by colony PCR using the primers listed in Table S10. The colony PCR results revealed the presence of the native *phaC1* locus in each clone by amplicons of 1.9 kb, along with other bands of undefined origin. For some clones, an additional band of 4.9 kb indicated a possible integration of the *appA* expression cassette (Figure S1). The presence of undisrupted wildtype locus in every clone suggests a common way to avoid the selection for genomic integration by kanamycin, suggesting the suicide plasmid might be maintained episomally.



**Figure S1: Colony PCR of *C. necator* H16 wildtype transformed with suicide plasmid pHInt-AppA-KanR-loxP.** An integration of the *appA* expression cassette into the *phaC1* locus via double crossover leads to an amplicon of size of 4.9 kb. Bands of 1.9 kb in size correspond to the undisrupted wild type *phaC1*.

We therefore performed another colony PCR with primers designed to only give a product with circular plasmid DNA as template (primer pSeq-phaC1\_f1/r1, see Table S10). Indeed, the corresponding agarose gel showed an amplicon of 1.5 kb for each clone, corresponding to the circular suicide plasmid (Figure S2).

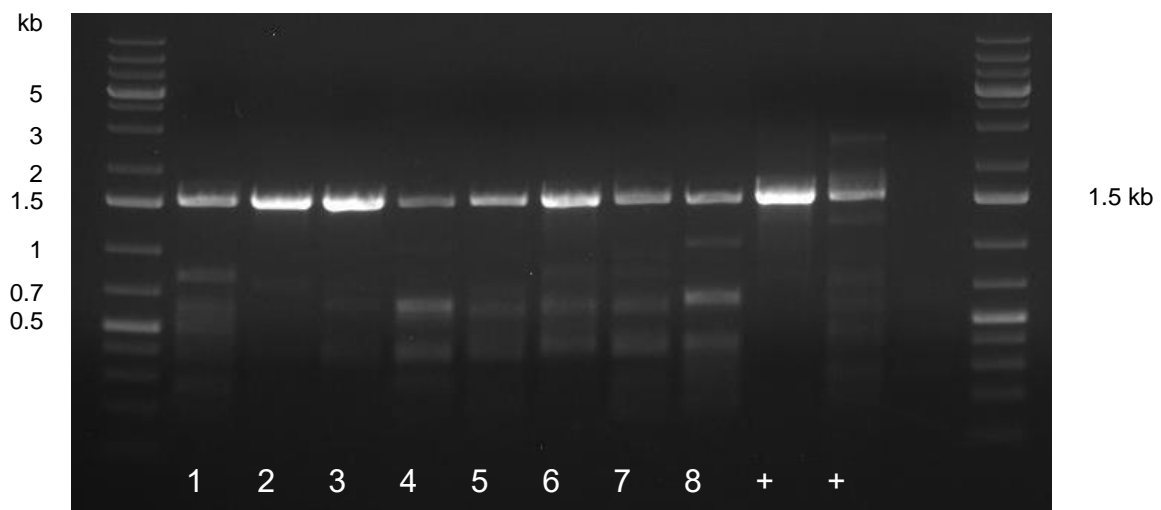


**Figure S2: Circular plasmid-specific colony PCR of mutants transformed with pHInt-AppA-KanR-loxP.** Primer amplifying a 1.5 kb fragment only in the presence of circular plasmid were chosen. (+) refers to the use of pHInt-AppA-KanR-loxP plasmid DNA as positive control, with two different amounts applied as template.

As we aimed for a clear integration into the locus with *phaC1* disruption, we decided to proceed with the linear *appA* expression cassette to avoid strain instabilities. The linear fragment was transformed into *C. necator* H16 wildtype as well as the *eGFP* expression strain. Successful integration was verified with colony PCR using the primers listed in table S10. Colony PCR results for multiple screened clones with a wild type (Figure S3) and a *eGFP* strain background (Figures S4 – S5) are shown below.

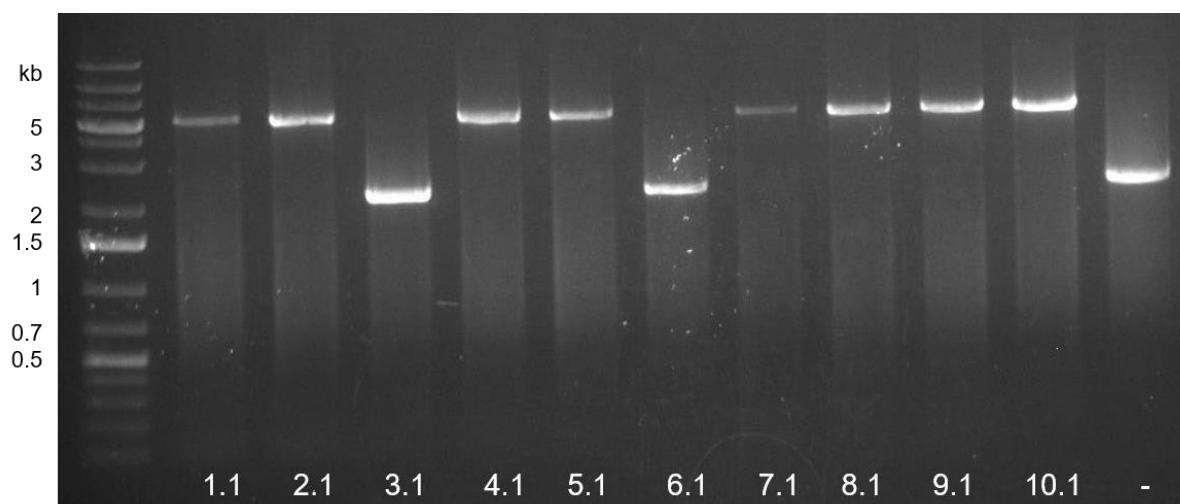


**Figure S3: Control PCRs of *C. necator* WT transformed with the linear pHInt-AppA-PhaC-loxP fragment.** Amplicons of 4.9 kb correspond to the target integration, amplicons at 1.9 kb correspond to the undisrupted native *phaC1* locus and therefore unsuccessful integration or negative control, respectively.

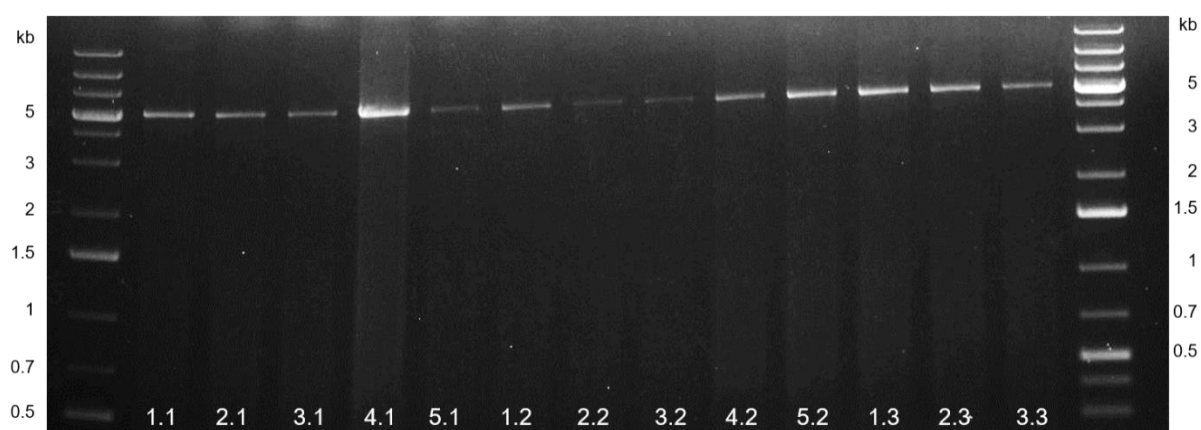


**Figure S4: Control PCRs of *C. necator* eGFP transformed with the linear pHInt-AppA-PhaC-loxP fragment.** Amplicons of 4.9 kb correspond to the target integration

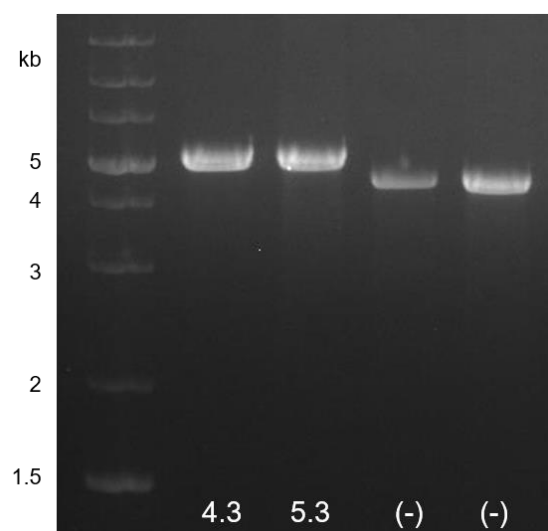


**Figure S5: Control PCRs of *C. necator* eGFP transformed with the linear pHInt-AppA-PhaC-loxP fragment including negative control.** The negative control correlates to the undisrupted *eGFP* locus with an amplicon size of approximately 4.3 kb while the integration of the *appA* cassette exhibits an amplicon of 4.9 kb.